ESPOO 2002 VTT RESEARCH NOTES 2163

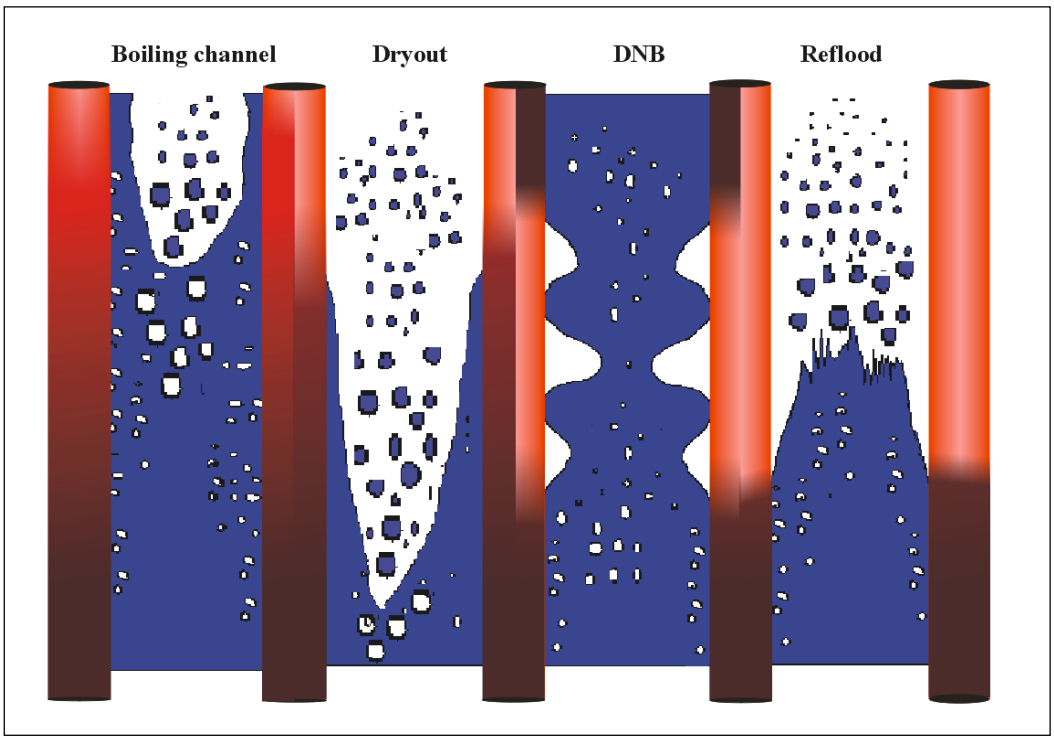

Jaakko Miettinen & Anitta Hämäläinen

GENFLO –

A General Thermal Hydraulic Solution for Accident Simulation

VTT TIEDOTTEITA – RESEARCH NOTES 2163

GENFLO –
A General Thermal Hydraulic Solution for Accident Simulation

Jaakko Miettinen

Anitta Hämäläinen

VTT Processes

ISBN 951–38–6083–3 (URL: http://www.inf.vtt.fi/pdf/)
ISSN 1455–0865 (URL: http://www.inf.vtt.fi/pdf/)

JULKAISIJA – UTGIVARE – PUBLISHER

VTT, Vuorimiehentie 5, PL 2000, 02044 VTT
puh. vaihde (09) 4561, faksi (09) 456 4374

VTT, Bergsmansvägen 5, PB 2000, 02044 VTT
tel. växel (09) 4561, fax (09) 456 4374

VTT Technical Research Centre of Finland, Vuorimiehentie 5, P.O.Box 2000, FIN–02044 VTT, Finland
phone internat. + 358 9 4561, fax + 358 9 456 4374

VTT Prosessit, Tekniikantie 4 C, PL 1604, 02044 VTT
puh. vaihde (09) 4561, faksi (09) 456 5000

VTT Processer, Teknikvägen 4 C, PB 1604, 02044 VTT
tel. växel (09) 4561, fax (09) 456 5000

VTT Processes, Tekniikantie 4 C, P.O.Box 1604, FIN–02044 VTT, Finland
phone internat. + 358 9 4561, fax + 358 9 456 5000

Technical editing Maini Manninen

Otamedia Oy, Espoo 2002

Miettinen, Jaakko & Hämäläinen, Anitta. GENFLO - A general thermal hydraulic solution for accident simulation. Espoo 2002. VTT Tiedotteita – Research Notes 2163. 75 p. + app. 4 p.

Keywords nuclear power plants, nuclear reactors, accidents, simulation, GENFLO, heat transfer, thermal hydraulics, coolants, loss of coolant accidents, dryout

Abstract

Thermal hydraulic simulation capability for accident conditions is needed as a part of several programs. Specific thermal hydraulic models are too heavy for simulation, because also the simulation of the rest of the system requires computer resources. The coupling between different physical models may be so complex that the fixed scope system codes are impossible to install for serving the special physical applications. Hence, the GENFLO (=GENeral FLOw) thermal hydraulic model has been developed at VTT for special applications. This report describes the generalised thermal hydraulic model, GENFLO, which at present has been used in three different applications. In RECRIT, the model is coupled the 2-D transient neutronics model TWODIN for calculating the recriticality accidents in the BWR plant. In FRAPTRAN application the model has been coupled with the transient fuel behaviour code FRAPTRAN for making the study of complex fuel transient possible by simulating the sub-channel thermal hydraulics as realistic as possible. In APROS-SA application the model calculates the core thermal hydraulics during the severe accident until the fuel material relocation and pool generation to the bottom of the reactor vessel is simulated.

Contents

List of symbols

A	Flow area, m^2
Bi	Biot's number,
C_0	Drift flux distribution parameter, -
C_N	Concentration of non-condensibles in vapour, -
C_{CR}	Concentration of control rods, -
c_l, c_g	Specific heat capacity of liquid and gas, J/kg/K
c_f, c_c	Specific heat capacity of fuel and cladding, J/kg/K
D_h, D_e	Channel diameter, hydraulic diameter, m
d	Droplet diameter, m
f_w	Wall friction loss
g	Constant of gravitation = 9.81 m/s^2
h_f	Wet side heat transfer coefficient (HTC) in the front, W/m^2K
h_{nb}, h_{fb}, h_{tb}	Nucleate, film and transition boiling HTC, W/m^2K
h_c	Convection HTC, W/m^2K
h_r	Radiation heat transfer coefficient, W/m^2K
h_g, h_l, h_s	Enthalpy of gas and liquid, saturation enthalpy, J/kg
i, j	Local, node or junction index
j_g, j_l, j_m	Superficial velocity of gas, liquid and mixture, m/s
J_g, J_l, J_m	Volumetric flow of gas, liquid and mixture, m^3/s
$K(T)$	Coefficient in Urbanic-Heidrich correlation, -
M_l, M_g	Liquid and gas mass, kg
o	Index old
P	Perimeter
Pe	Peclet's number, -
Pr	Prandtl number, -
p	Pressure, Pa
q''	Heat flux per surface area, W/m^2
q'''	Heat flux per coolant volume, W/m^3
q_g, q_l	Heat flux from wall to gas and liquid, W/m^2
q_w	Heat flux from wall, W/m^2
q_{nb}, q_{fb}, q_{tb}, q_{if}	Nucleate, film, transition boiling and interfacial heat flux, W/m^2
Q_g, Q_l	Heat source to gas and liquid, W
Re_l	Reynolds number, -
s_g, s_l	Liquid, steam source, kg/m^3s
S_g, S_l	Liquid, steam source, kg/s
S_w	Perimeter of structure, m
Δt	Time step, s
T_g, T_l, T_s	Gas, liquid and saturation temperature, ^oC
T_c, T_f	Cladding and fuel temperature, ^oC

T_0	Leidenfrost temperature, $T_0=\Delta T_{Leid} + T_s$
t	Time, s
u_g, u_l, , u_m	Velocity of gas, liquid and mixture, m/s
V_{gj}	Drift flux velocity, m/s
V_{fr}	Quench front velocity, m/s
V_i	Node volume
W_g, W_l, W_m	Mass flow rate of gas, liquid and mixture, kg/s
x	Steam quality, -
X_k	Pressure singular loss coefficient, -
z	Coordinate in axial direction

Greek symbols

α	Void fraction
ε_w, ε_l	Emissivity of wall and liquid
γ	Mass transfer, kg/m^{3}s
Γ	Mass transfer, kg/s
λ_l, λ_g , λ_w	Thermal conductivity of water, steam and wall, W/m/K
μ_l	Dynamic viscosity of water, kg/ms
ρ_g ,ρ_l, ρ_m	Density of gas, liquid and mixture, kg/m^3
σ	Stefan-Boltzmann constant = 5.7x10^{-8}
σ	Surface tension, N/m

SI units if not otherwise specified

1. Introduction

Simulation of the thermal hydraulic behaviour nuclear reactors during accident conditions has been a challenge since 1970. The first challenges were related to the rapid blowdown depressurisation during the large break LOCA, refill of the reactor vessel after the blowdown period by considering the multidimensional coolant bypass in the downcomer region, mainly based on the coolant injection from the hydro-accumulators, and finally the core reflooding period by low pressure coolant injection. The first system codes were developed for these simulation needs, but due to poor numerical schemes and slow computation capabilities the computation of these accidents was very time consuming. The length of the blowdown period was typically less than 100 seconds and special numerical treatment was needed due to rapid system pressure change and large pressure differences between different sections. It could happen that completely different codes were developed for the reflooding period of the large LOCA. In this period the system pressure changes were rather slow, but the reflooding physics was very complex and in the vicinity of the quenching front there was a need to consider the large temperature gradients in the fuel rods inside few millimetres. For the reflooding period the simulation of the vessel section could be enough.

After TMI-2 accident the interest was more focused to small break LOCA accidents and PSA studies of the effect of plant components and human errors. In these accidents the gravitational phase separation is an important contributor to the coolant distribution over the whole reactor system, coolability of the core and functionability of the steam generators or coolant dump to remove the generated energy. The simulation of these accidents was originally tried by using the large LOCA codes, but the computation of the accidents over a period of thousands of seconds was too time consuming. That is why a new generation of system codes was developed with an improved numerical solution and capability to use longer time steps, 0.1 seconds in stead of 0.001 seconds typically in large LOCA codes. In addition to system codes with rather long computation times another generation of codes was developed with capability to the real time calculation and these codes could already be used in the real time training simulators.

In parallel to the codes simulating thermal hydraulic events another generation of codes was developed for simulating the severe accident conditions leading to cladding rupture due to the oxidation, cladding melting in higher temperatures, fuel pellet relocation after the cladding damage and fuel melting, when temperatures are high enough. Similarly with thermal hydraulic system codes also the severe accident codes were rather time consuming. Due to complexity of the physical events the development of the severe accident codes was strongly coupled to the plant specific experiments.

A new phase of diversification started after the Chernobyl accident. Although the similar accident is not relevant in the traditional light water reactors, the possibility for reactor core re-criticality became interesting and both the delayed and prompt criticality was considered. To satisfy this interest a new need in the development of the analysis tools was created. It was realised that no system codes describes the physics in a sufficiently detailed manner, especially for the multidimensional neutronics. On the other hand the traditional core neutronic models were not sophisticated enough to simulate two-phase conditions in the main circulation systems. The need was solved by combining together the core part of the multidimensional neutronic model and loop model with two phase simulation capability. At VTT the SMATRA and HEXTRAN were examples of such combined program products.

Typical fuel analysis models include a complex physical description for the fuel rod pellet behaviour with thermal and structural mechanistic parameters. The weakest part in these codes could be the thermal hydraulic sub-channel description, if accident conditions with boiling are examined. The more advanced analyses require an improved thermal hydraulic model and closer coupled to the simulation of the accident itself.

More diversification can be expected, when the simulation tools are more developed for the two-phase CFD applications.

The thermal hydraulic model was originally developed for simulating thermal hydraulics of the RECRIT re-criticality code. With this application the well tested features of the two-dimensional dynamical neutronic model could be tested easily. Several years later there was a need to develop a more sophisticated sub-channel thermal hydraulic model to be coupled with the FRAPTRAN fuel code. In this application the complex fuel dynamical behaviour can be studied in accident conditions calculated with e.g. LOCA codes. As the latest application the same thermal hydraulic model was installed to the APROS engineering simulator for serving the operator training in severe accident conditions. In this application the real time severe accident simulation will be possible. After first RECRIT application the code has been necessary to be revised into the generalized direction. This report describes this generalized version of the GENFLO code.

2. Multipurpose thermal hydraulic simulation

2.1 System alternatives and basic principles

The thermal hydraulics solution principles of GENFLO are based on the models developed for the SMABRE (Miettinen, 2000a) for simulating thermal hydraulics during small break LOCA and large break LOCA conditions. In connection with 1-D core model TRAB and 3-D core model HEXTRAN the code has been used for analysing ATWS accidents. GENFLO thermal hydraulics is strongly simplified from that of SMABRE. But additional new features, reflooding heat transfer description, zirconium oxidation, radiation heat transfer and control rod melting model extend the applicability for simulation of severe accidents.

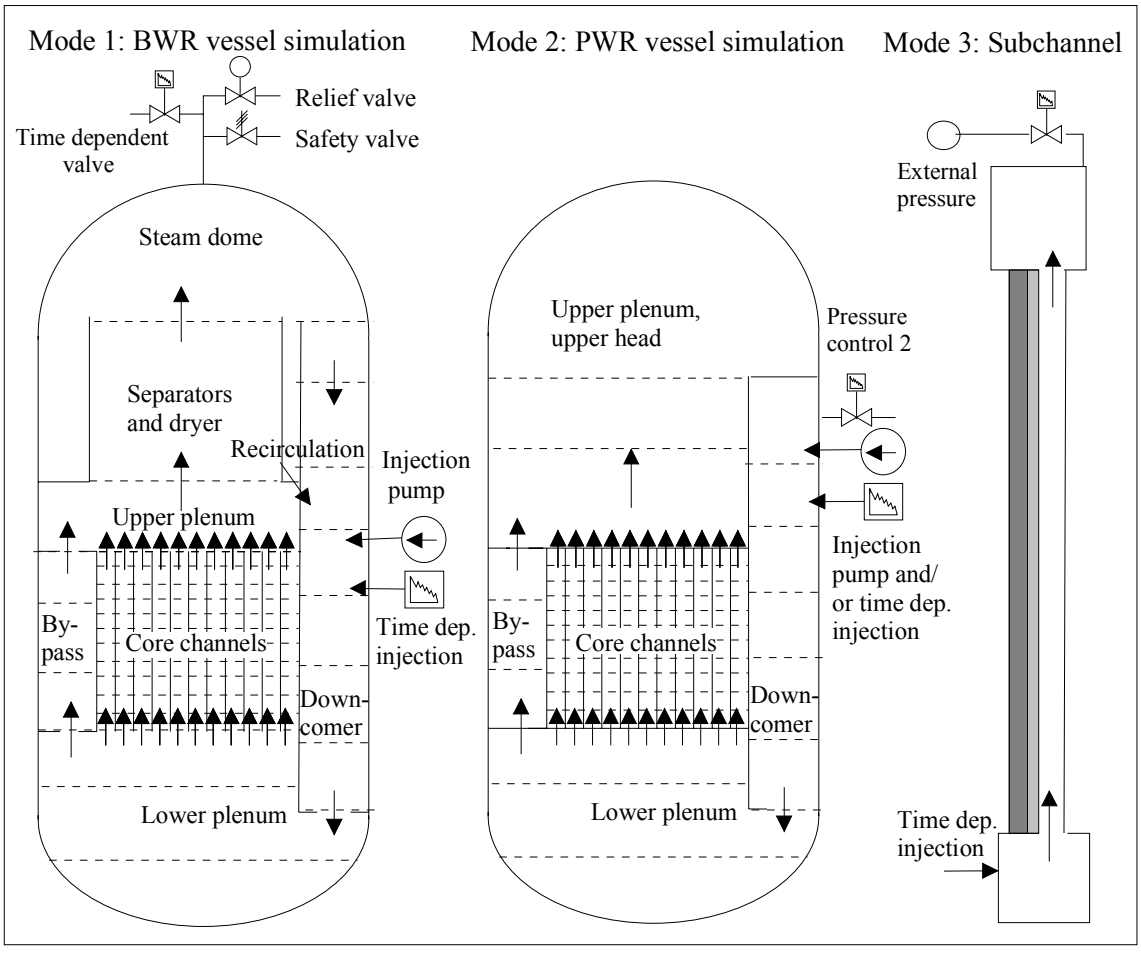

Figure 1. Alternative system concepts for the thermal hydraulic description in GENFLO.

In the generalized GENFLO concept the widest application requires the whole BWR or PWR vessel to be described. The most limited application describes only a single

subchannel of a fuel element, without any flow mixing with the neighbouring channels. The original geometry concept was strictly related to the BWR vessel geometry. After the extension of the scope the BWR vessel, PWR vessel and the single subchannel can be described by the same model.

The system simulation modes may be described as follows:

Mode1: In RECRIT application, the whole BWR reactor vessel is simulated with the core, bypass, upper plenum, separator, steam dome, downcomer and lower plenum. Typical BWR facilities for the pressure level and coolant inventory control are available. The concept is mainly aimed for BWR recriticality simulation. The system pressure is completely controlled by the valves connected to the steam dome. If the specific pressure is required for the simulation of experimental facilities, these conditions can be achieved with the time dependent valve. Anyhow, the model allows rather flexible modifications through input parameters and for example all validation cases for reflooding have been calculated by using this modelling concept.

Mode 2: This mode is especially for the APROS-SA application, when the PWR reactor vessel of VVER-440 type is described. The main boundary conditions are two pressures, one in the upper plenum due to the hot leg outlet and another on the top of the downcomer, due to the cold leg inlet. Both the upper plenum and downcomer may include coolant injections, but safety and relief valves are located in the upper plenum. The coolant may leak out from both the upper plenum and top of the downcomer. The basic assumption for the initiation of the simulation is that water level exists at least in the upper plenum. Later during the transient it is assumed that the water level is created also into the downcomer. In addition to that only such simulations are relevant, where external pressure node is assumed to contain non-condensable gas or steam and the flow towards the system contains so only gas.

Mode 3: This mode is very practical in FRAPTRAN subchannel simulation and in validation against small channel experiments, where the system pressure is fixed inside narrow margin and coolant is injected into the bottom of the test section. The calculated coolant leak out is mainly from the upper plenum. The main boundary conditions are pressure in the upper plenum and the upper plenum and lower plenum injections or leaks. Safety and relief valves locate in the upper plenum.

Mode 4: This mode is an alternative mode in FRAPTRAN subchannel simulation, where the external calculation model supplies the pressures in upper and lower plenum for boundary conditions. The presumption of this mode is that the boundary conditions of lower plenum may include coolant flow in, not out. The coolant properties are specified for the external pressure node. The upper pressure boundary condition may

include the inflow and outflow. This mode is rather difficult to be used for simulating experimental facilities, because the flow through the test section is not typically controlled by the pressure difference over the test sections.

The thermal hydraulic input data in all applications has been minimized by hard-wiring the nodalization to lumped sections. The user defines the geometrical data only for these major volumes. The calculation level subdivision of nodes is generated automatically based on the given number of nodes inside each major volume. The initialization creates the calculational level nodalization. The calculation level components include the nodes, the junctions connecting nodes and heat structures with a solid wall connected to the node. The thermal hydraulic components on the calculational level are the nodes, junctions and heat structures. The node geometry on the calculational level is defined by the node area, length, elevation and equivalent diameter. The thermal hydraulic state is determined by pressure, steam mass, water mass, water enthalpy, steam enthalpy and concentration of noncondensables. From these values the calculated quantities are extracted including the void fraction and water level. The junction geometry is defined by flow area, elevation and friction coefficient. Thermal hydraulics in a junction is defined by liquid mass flow and steam mass flow. During the calculation the mixture volume flow is an important parameter.

The basic field equations in GENFLO include the mass conservation equations, one mixture momentum equation between parallel channels and two energy equations. The phase separation and the velocity difference between the phases are obtained from the drift flux model. The basic variables in the thermal hydraulic solution are the pressure, void fraction, mixture velocity, gas enthalpy, liquid enthalpy, and concentration of noncondensables. The solution is realized by using the principle of the integral momentum equation in three steps:

1. The system pressure is solved based on the balance between coolant inflow, coolant outflow, energy addition and by assuming vapour density and saturation temperature to be functions of the system pressure only. The inlet flow into individual flow channels is solved from the integral momentum equation and the mixture velocity is solved from the flow injections, integral momentum and local vapour generation.

2. The phase separation is solved using the drift-flux model and giving the mixture flow split into the phase mass flow rates, and

3. Solving for enthalpies of liquid and vapour.

The principle of integral momentum equation includes the integration of the system pressure above the channel and of the inlet velocities into the individual parallel flow

channels. Then with assumptions related to vapour densities, the mixture flow distribution is fixed for the whole system. The local pressure includes an effect of the dynamic flow friction and a gravitational term. The dynamic pressure loss is used only for the core inlet flow distribution, not for the vapour density and saturation temperature. The gravitational pressure loss may be taken into account for the vapour density and saturation temperature. The local pressure is a sum of the system pressure and the pressure losses due to friction and gravitation.

The heat transfer model accounts for the wetted wall heat transfer below the dryout point / quench front, dryout position moving downwards or the quenching front moving upwards. The post-dryout heat transfer is solved above the dryout position / quenching front.

The dryout is based on a dryout correlation. The quenching front propagation is calculated by using an analytical model for the conduction controlled rewetting. Below the quench front, the heat transfer is due to nucleate boiling and forced convection. The heat transfer mechanisms in the post-dryout regimes: transition boiling, film boiling, convection, interfacial heat transfer from superheated steam to water droplets, and radiation heat transfer to water droplets are considered simultaneously and their individual contributions are weighted using appropriate efficiency multipliers. These multipliers have been determined in the validation process.

For the film boiling, the Bromley film boiling correlation is used. The transition boiling, where the liquid contacts the wall periodically, is approximated as a linear interpolation from critical heat flux to minimum film boiling heat flux. The critical heat flux is calculated from a separate model combining pool boiling critical heat flux with a non-linear void correction. The gas heating is calculated by the Dittus-Boelter correlation. The interphasial heat transfer between the superheated vapour and liquid is calculated from the heat transfer analogy for spheres surrounded by the gas.

At high temperatures, the cladding oxidation creates an additional heat source and results in hydrogen generation. The zirconium oxidation reaction rate is described by a parabolic expression with reaction rate coefficient, time and extent of reaction. The reaction rate coefficient is temperature dependent. It is expressed by an Arrhenius equation. The coefficients of the oxidation model are based on the proposal of Urbanich and Heidrich. The oxidation rate is limited with the steam starvation.

Thermal hydraulic solution principles and the heat transfer model of GENFLO have been developed on the basis of the RECRIT code. The validation cases for the RECRIT code includes ERSEC, ACHILLES, REWET-II, GÖTA, FLECHT and QUENCH experiments.

2.2 RECRIT application of GENFLO

The RECRIT computer code is based on joint inter-Nordic work between Risø and VTT (Miettinen et al, 2000b). The code combines a neutronics model, based on a two-dimensional cylinder symmetric core description, with a thermal hydraulic model GENFLO, Fig. 2.

The real pressure vessel includes the downcomer, lower plenum, core, bypass, upper plenum, steam separator and the steam dome. Because the model is simulating the conditions only after the reactor scram and pump trip, the forced flow conditions with the dynamics of recirculation pumps and steam separators are not described. The sections outside the core are defined as one-dimensional components. The user defines integral data for bypass, upper plenum, steam separator, lower plenum, downcomer and steam dome.

Only necessary boundary conditions are described for water injections, HPCIS as a time dependent injection and LPCIS as a pressure dependent injection. The pressure dependent injection is defined by a quadratic polynomial curve. For steam release from the vessel the time dependent valve, the relief valve by a ramp opening characteristics or a safety valve by a hysteresis characteristics may be defined. These choices may be used for the description of the constant pressure control, over-pressure protection and ADS depressurization.

The RECRIT core is described by a two-dimensional model, cylindrically symmetric geometry using typically 10–100 axial nodes and 3–20 radial rings for the real plant core. The neutronic nodes are related to fuel rod heat structures. The thermal hydraulic nodalization may be as dense as in the neutronics model, but the model allows also a less dense thermal hydraulic nodalization. The thermal hydraulic part is the most time consuming in this application, thus the computing time may be reduced by modifications in nodalization. The radial rings have an equal thickness, not an equal flow area. This choice is due to the fact that for the neutron diffusion the distances are most important. The variable mesh length in radial or vertical direction may worsen the numerical convergence. The time integration is based on the forward Euler- method. In the most critical phase of the accident the neutronics model may require the time steps of 0.1 ms. In these situations the thermal hydraulic timestep is typically limited to minimum 0.01 seconds and the neutronic model is repeated during a single thermal hydraulic time step until the timestep has been accumulated.

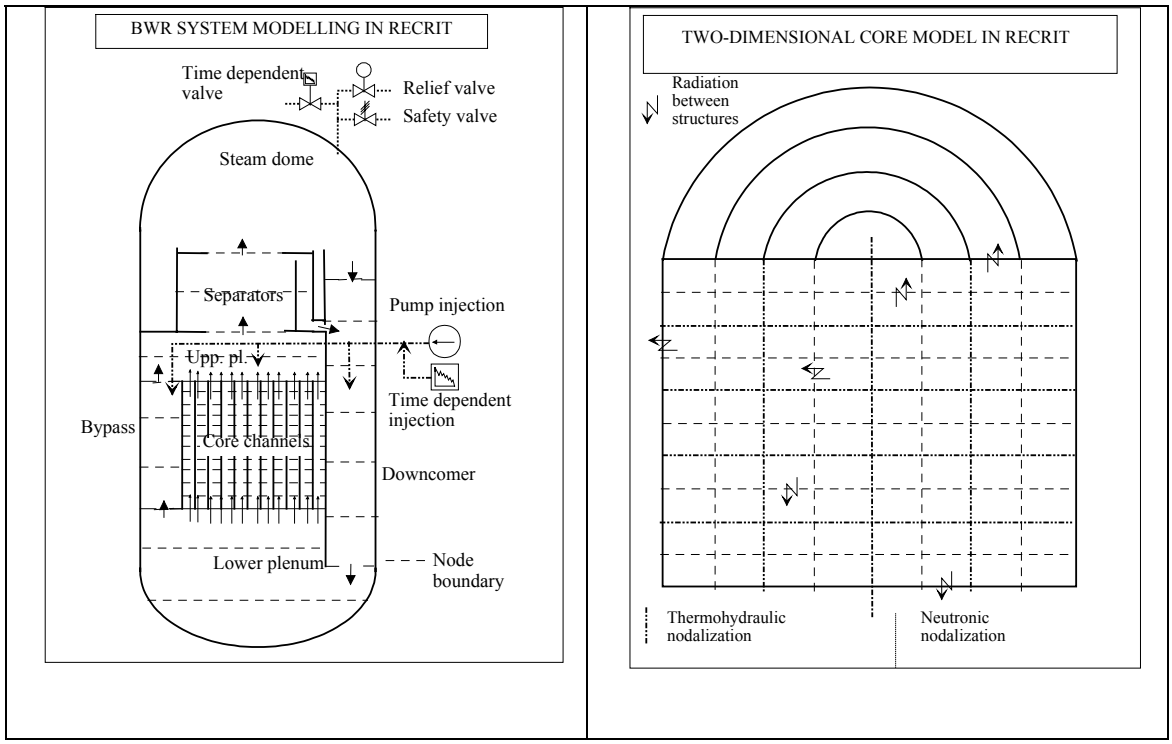

Figure 2. BWR processes and two-dimensional neutronics described in the RECRIT application.

In the axial direction both the neutronics (heat structure) nodes and thermal hydraulic nodes have an equal length. The schematic presentation of the two-dimensional core is depicted in Figure 2.

The fuel heat structure is defined by cladding area, pellet area, gas gap thickness, cladding volume and pellet volume. The neutronic calculation mesh points are related to the fuel structure mesh points. The fuel bundle shrouds (boxes) and grid spacers are not included in the model. The radial temperature profile or just average temperatures are solved in the cladding and fuel pellet. The reactor vessel steel structures and the reactor vessel walls are not modelled.

The decay heat and the fission power of the fuel pellets is integrated by the heat conduction model, which integrates the fuel pellet, the gas gap and the cladding structure for getting the Doppler effect on the neutronics solution. The heat generation rate (fission and decay heat) determined by the neutronics model is transferred to the thermal hydraulic part of the code as a heat source of the fuel pellet. The thermal hydraulic model calculates also the heat generation from zirconium oxidation reaction in the cladding. The oxidation of fuel boxes is not accounted for. The control rod melting is simulated assuming the temperature of a control rod to follow closely the

temperature of the fuel rods. The thermal hydraulic part of the code calculates the radiation heat transfer between heat structures in axial and radial directions as well as the radiative heat losses from the peripheral zones to the surroundings.

Combining two separate codes, developed physically at different locations is some kind of the art of science. The initial neutronics model included a model for fuel rod temperatures. Based on earlier experiences defining the boundary between codes on the cladding surface was not seen as a good approach, because both the cladding and fuel temperature depend very strongly on the heat transfer on the cladding. That is why the thermal hydraulic simulation was expanded from the coolant to the heat structure integration. By this approach the parameter transfer between the thermal hydraulic and neutronics part may be depicted as shown in Figure 3.

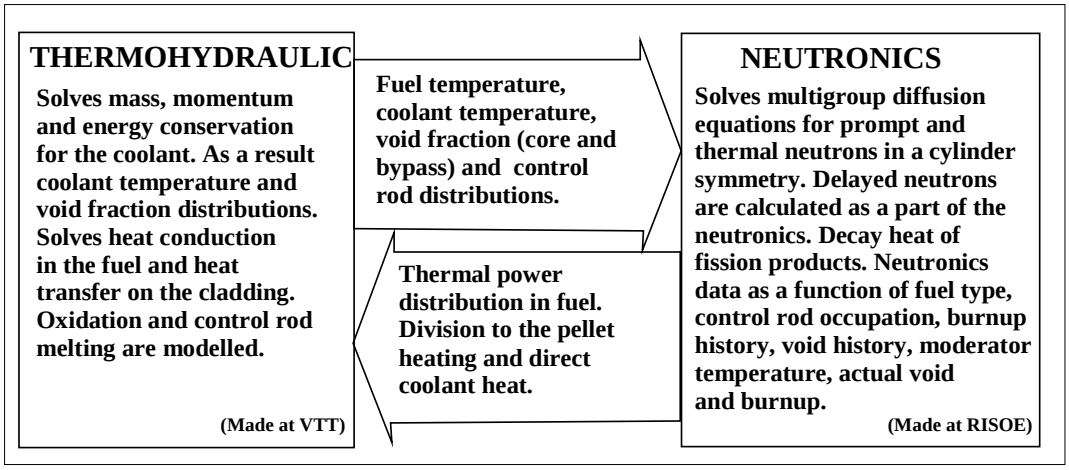

Figure 3. Change of information between the GENFLO thermal hydraulics and TWODIM neutronics.

2.3 FRAPTRAN application of GENFLO

The fuel performance in accident conditions can be analysed at VTT e.g. with the FRAPTRAN code (Cunningham et al., 2001), developed by USNRC. Its fuel rod models have recently been upgraded. In order to provide feedback from FRAPTRAN to thermal hydraulics during transients, the coupling of FRAPTRAN and GENFLO codes have been performed (Hämäläinen et al., 2001a). Especially in fast changing transient conditions like the ATWS in BWR plants this has shown to be necessary (Hämäläinen et al., 2001b). In these transients the hot channel and also the whole core may experience transitions from the wetted state to the dry state and back and the fuel structure experiences strong loadings. That is why it is relevant to consider the fuel behaviour in oscillatory temperature conditions.

The system behaviour and boundary conditions needed for the detailed core simulation and study of the fuel rod behaviour in FRAPTRAN-GENFLO analyses may be calculated with various codes, like the system code RELAP5, three-dimensional BWR or PWR reactor dynamics codes TRAB-3D (Daavittila & al., 2000) or HEXTRAN (Kyrki-Rajamäki, 1995), fast-running small break LOCA and ATWS analysis model SMABRE or the engineering simulator APROS (Puska, 1999).

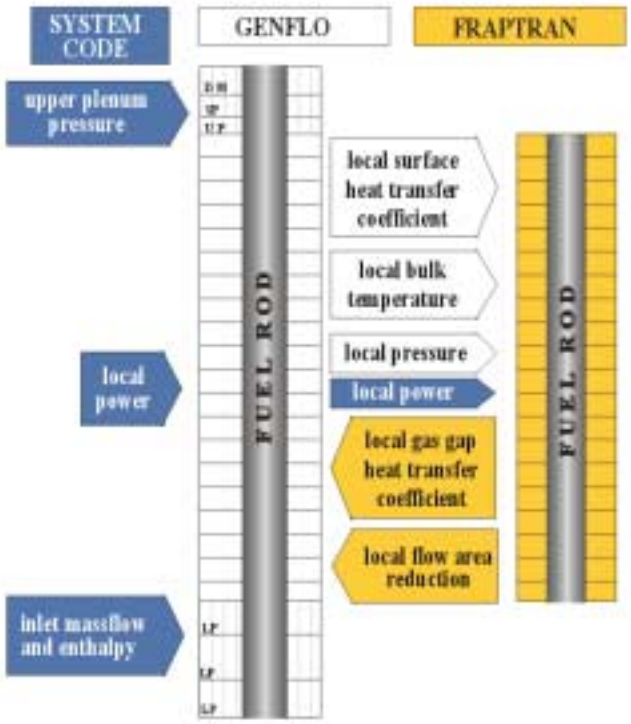

Figure 4. Typical sub-channel nodalization and data change between system code, GENFLO and FRAPTRAN.

In GENFLO, the coolant mass, momentum and energy conservation are solved for single flow channel, including the calculation of fluid temperature and void fraction distributions. As the result, the fluid temperature and heat transfer coefficient for each axial level at each time step have been supplied for the FRAPTRAN code. Data change between the codes is depicted in Figure 4. In addition to the fluid flow calculation, the GENFLO model includes an own solution for the transient temperature behaviour in the fuel rod. The oxidation of the cladding and the hydrogen generation consequently are calculated. The oxidation is an additional heat source, and the hydrogen is an important limiter for the oxidation. The FRAPTRAN includes in parallel to GENFLO an own solution of the heat conduction equations and it calculates temperatures and deformation of the fuel pellets and cladding, including ballooning, with an initial burnup. The axial power profile is given as the boundary condition for the thermal hydraulic model. The

axial mesh division of the fuel rods for both the codes is the same. In the radial direction of the core, several parallel channels and fuel rods may be described in GENFLO.

The coupling of the FRAPTRAN and GENFLO parts includes overlapping with respect to the fuel rod. Own fuel rod heat conduction and oxidation models exist in both codes. An alternative solution would include a sharp boundary on the cladding surface, with solid temperature calculated by FRAPTRAN and fluid temperature by GENFLO. This approach includes a risk for the numerical instabilities and distortion of the energy balance. With the selected approach these problems may be avoided. The method with using partial overlapping has been successfully applied at VTT for coupling the system thermal hydraulic model with the multidimensional core model for the reactivity accident and ATWS calculations.

2.4 APROS-SA application of GENFLO

The APROS-SA application of the GENFLO model is a part of the APROS training simulator (Lundström et al., 2001). A special relocation model, SARELO (Miettinen et al., 2002), has been designed for the reactor core describing the core overheating, oxidation, cladding melting, fuel relocation, control rod melting and finally fuel melting. SARELO calculates only one temperature for each core node, without dividing the cladding and fuel pellet. This is sufficient while starting the simulation in decay heat conditions. After lower support plate failure the molten core is relocated to the lower plenum and the conditions are simulated by the COPOMO (COrium POol MOdel) model. The model considers the molten core fragments as single mass and temperature nodes, but special nodalization has been applied for simulating the heat transfer though the vessel wall and melting of the wall. For the simulation the release of the fission products from the core and their transport in then primary loop a special module FIRPOMO has been developed. The fluid filled volume changes during the core relocation and this feature is considered in GENFLO. The concept considered for the severe accident scenarios is depicted as simplified in Figure 5. The phases during the progress of such an accident are depicted in Figure 6, including

I. the plant operation in nominal conditions,

II. the core heatup as a consequence of the core uncovery, the hydrogen generation begins in this phase,

III. the relocation of the overheated core, when the cladding is melting and flowing downwards and later the uranium oxide is melting as well and relocated downwards

IV. the pool formation at first inside the core barrel and after the barrel wall wall has been punctured, the formation of the new pool into the lower plenum.

basic concept for simulating the severe accident in the APROS-SA simulation are depicted in Figure 6. scenarios of such an accident are details in the APROS-SA simulation concept have been depicted in Figure 6.

The pressure boundary conditions are defined for the upper plenum and top of the downcomer. Both the upper plenum and downcomer may include coolant injection as boundary conditions. During simulation GENFLO supplies to APROS the liquid and steam outflow and enthalpies of outflow as well the hydrogen content of the flow.

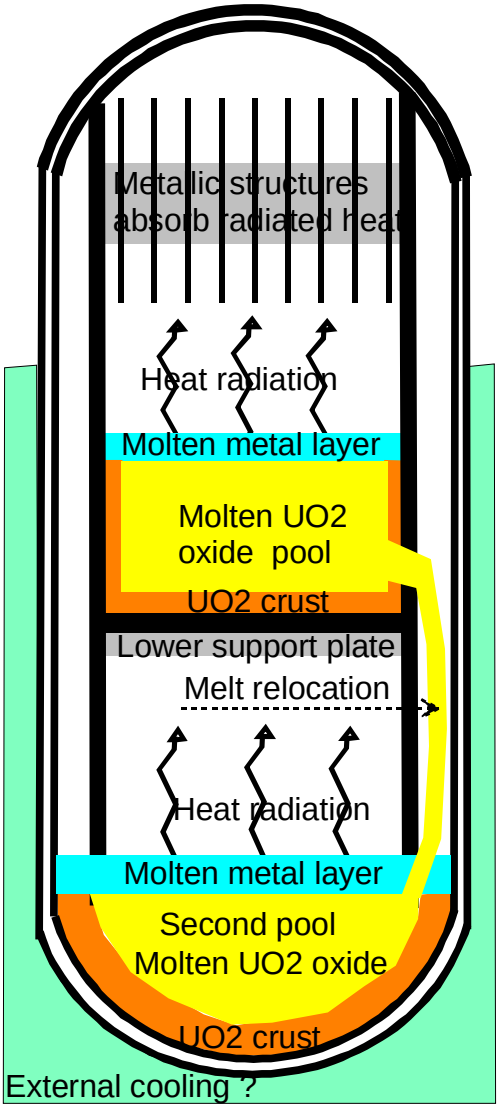

Figure 5. The concept in describing the severe accident scenarios in the APROS-SA application of the GENFLO thermohydraulics.

The SARELO model simulates all physical and mechanistic behaviour related to the fuel rods, control elements and lower core support plate. Initially the material are solid, but during the transient they can melt. The radiation and conduction heat transfer between zones is simulated as well. GENFLO calculates the heat flux from the structures to the coolant. The cladding oxidation and heat transfer between the fuel and control elements is solved in SARELO. After all heat transfer components are adjusted, the structure temperatures are integrated in the SARELO model. After the fuel and control element material begins melting, it is relocated to the lower levels. The UO_2 relocation gives a new shape for the power profile as well.

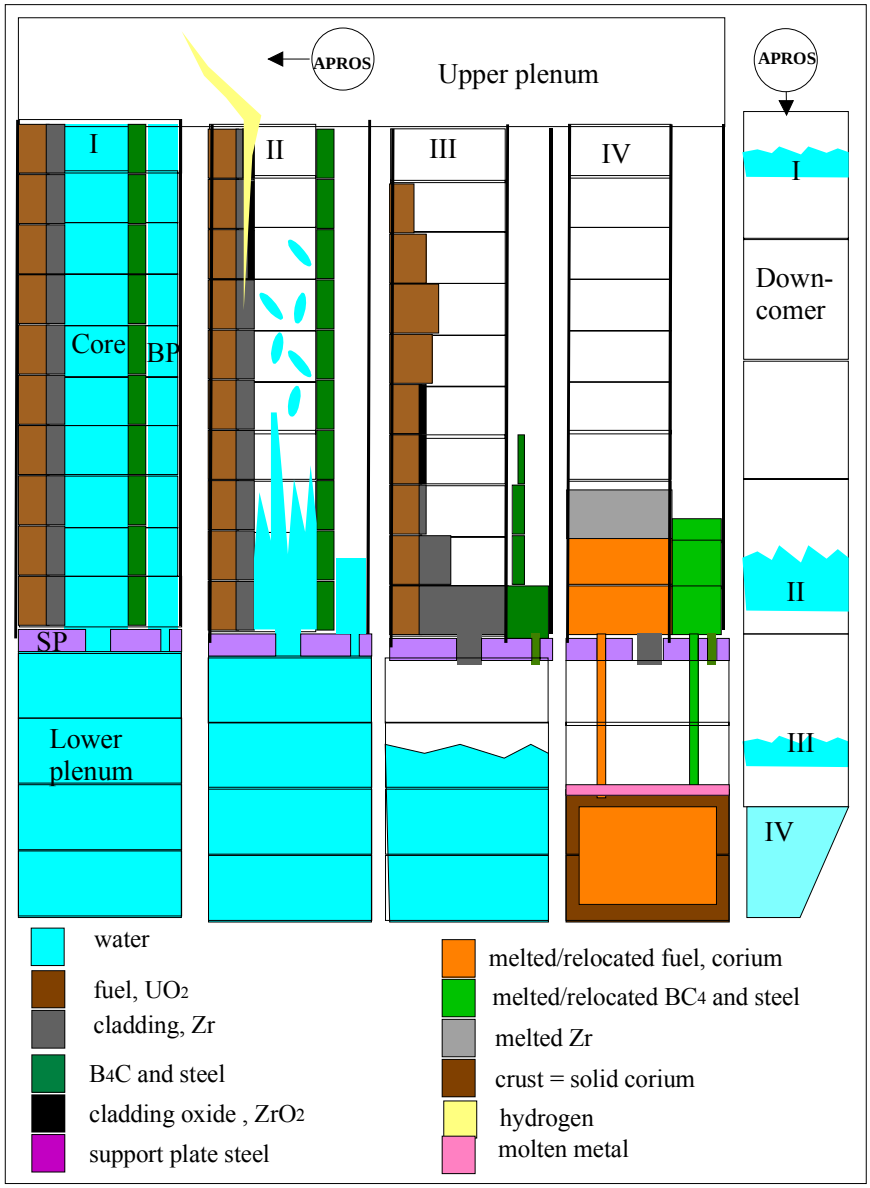

Figure 6. The phases of the severe accident scenarios in the APROS-SA application for the Loviisa power plant.

The share of the simulations tasks and the parameter interface between GENFLO and other modules in the APROS-SA –application has been depicted in Figure 7.

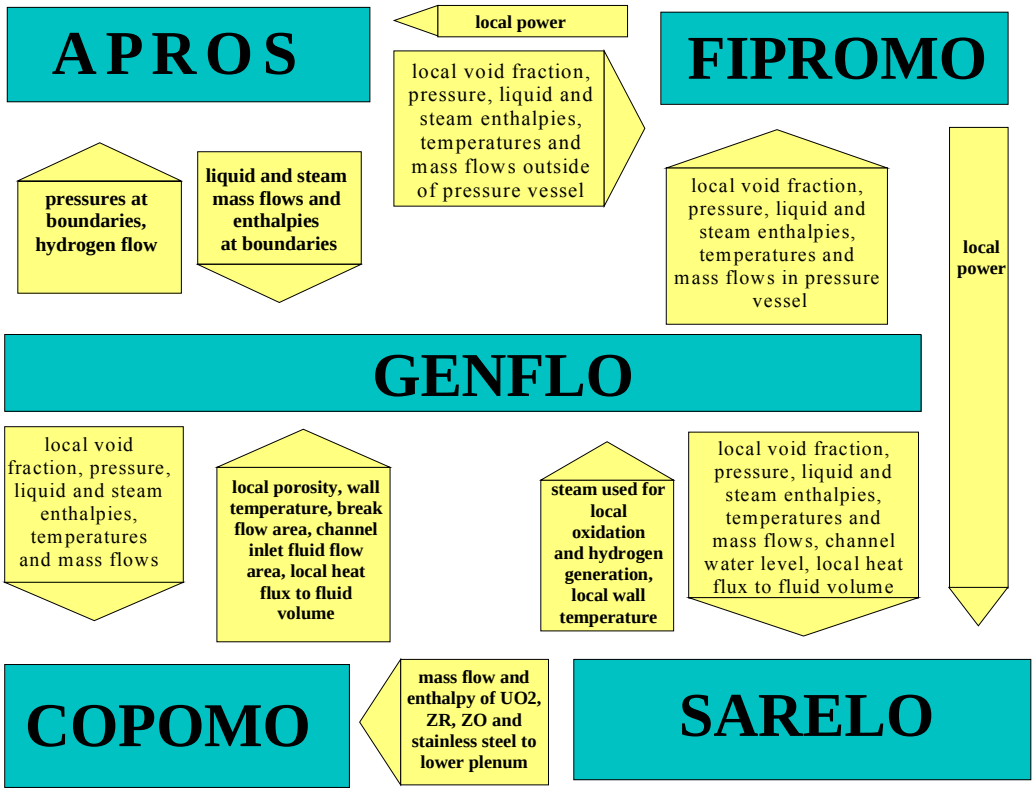

Figure 7. The share of the simulation tasks and the parameter interface between GENFLO and the other modules in the APROS-SA severe accident simulation.

The molten core mass transfer in the lower part of core is an input for the molten pool model COPOMO, which calculates also the core relocation into the lower plenum after the lower core support plate failure or through hole in crust. COPOMO has an interface with GENFLO, too, in the form of the cooling of the melt pool by possible coolant injection and reductions of fluid flow area.

3. GENFLO thermal hydraulic model

3.1 Principles of solving conservation equations

The basic conservation equations for the thermal hydraulic solution are written for liquid and steam mass conservation, mixture momentum conservation and liquid, steam energy conservation and concentration of noncondensables in vapour. The solution has been simplified into the integral momentum principle.

The principles of the further solution may be described as follows:

- The phase separation is solved by a drift flux model.
- For the pressure loss smooth wall friction and singular pressure loss in contractions are accounted for.
- The wall heat transfer correlations cover the whole heat transfer regime map from single phase convection into subcooled liquid to the single phase convection into superheated steam. The quenching front movement is solved using a mathematical model. The radiation heat transfer, oxidation and control rod melting are considered, too.
- The interfacial heat transfer between liquid and steam comprises condensation, when the two-phase mixture liquid is subcooled, flashing, when liquid is superheated and energy transfer from superheated steam to droplets. The condensation on subcooled walls is calculated as well.
- The conservation equations of the noncondensable gases in vapour can be integrated.

3.2 Basic conservation equations

Equations (3.1)–(3.5) are the basic conservation laws applied in the GENFLO thermal hydraulic model.

Mixture mass conservation equation

$$\frac{\partial(A\rho_m)}{\partial t} + \frac{\partial(W_m)}{\partial z} = As_l + As_g \qquad (3.1)$$

Equation (3.1) defines the mixture mass conservation. The equation is used in four steps: First the system pressure in the vessel is calculated based on the mass balance changes and compressibility of the mixture. After the integral momentum solution the volumetric flow distribution is defined around the circuit. After defining the phase separation by the drift flux model, the phasial liquid and steam masses are determined. Finally, the mass conservation is integrated for the individual nodes.

Mixture momentum conservation equation

$$\frac{\partial}{\partial t}W_m + \frac{\partial}{\partial z}\frac{1}{A}\frac{W_m^2}{\rho_m} = -A\frac{\partial p}{\partial z} - A(\frac{\partial p}{\partial z})_f - A\rho_m g\cos\theta \tag{3.2}$$

The momentum Equation (3.2) is applied in two steps: The circulation rate is solved from the integral momentum integrated over the loop. An integral momentum equation is solved for the core inlet into each radial channel, into bypass and for the recirculation backflow. After the volumetric flow rate in these junctions is fixed, the volumetric flow distribution around the circuit may be determined. After the local mass flow rates have been determined, the momentum equation is used for calculation of pressure distribution around the circuit.

Gas enthalpy conservation equation

$$\frac{\partial}{\partial t}(A\rho_g h_g) + \frac{\partial}{\partial z}(W_g h_g) - A\alpha\frac{\partial p}{\partial t} = h_{g,i}As_g + Q_g \tag{3.3}$$

Liquid enthalpy conservation equation

$$\frac{\partial}{\partial t}(A\rho_l h_l) + \frac{\partial}{\partial z}(W_l h_l) - A(1-\alpha)\frac{\partial p}{\partial t} = h_{l,i}As_l + Q_l \tag{3.4}$$

The energy Equations (3.3) and (3.4) for liquid and for steam, respectively, are integrated after the local mass flow rates are determined. For the energy equation the donor cell discretisation is applied and to avoid matrix inversions, integration is performed from node to node following the nominal flow direction.

Conservation of the non-condensable fraction, hydrogen or nitrogen in the gas gives

$$\frac{\partial(A\alpha\rho_g C_N)}{\partial t} + \frac{\partial(A\alpha\rho_g u_g C_N)}{\partial z} = As_g C_{\mathrm{N,gi}} \tag{3.5}$$

The Equation (3.5) is solved for the concentration of non-condensables in GENFLO applications they include nitrogen from accumulator water and hydrogen from zirconium oxidation.

The relations between different thermal hydraulic parameters are collected into Table 1. These relations are used, when the equations are developed for further solutions.

The phase separation has been described by using the drift flux model, where the basic formula known as Zuber-Findlay drift-flux model may be defined by

$$u_g = C_o\, j_m + V_{gj} \tag{3.6}$$

Table 1. Basic relations between different thermal hydraulic parameters.

Expression	Meaning
$M_g = \alpha V \rho_g = \alpha(\Delta z\, A)\rho_g$	Gas mass in a volume, kg
$M_l = (1-\alpha) V \rho_l = (1-\alpha)(\Delta z\, A)\rho_l$	Liquid mass in a volume, kg
$W_l = u_l A \rho_l$	Liquid mass flow, kg/s
$W_g = u_g A \rho_g$	Gas mass flow, kg/s
$W_m = W_g + W_l$	Mixture mass flow, kg/s
$u_m = \alpha u_g + (1-\alpha) u_l$	Mixture velocity, m/s
$\rho_m = \alpha \rho_g + (1-\alpha)\rho_l$	Mixture density, kg/m^3
$j_m = j_g + j_l = u_m$	Superficial mixture velocity m/s
$j_g = u_g \alpha$	Superficial gas (drift) velocity, m/s
$j_l = u_l (1-\alpha\ )$	Superficial liquid (drift) velocity, m/s
$u_r = u_g - u_l$	Relative velocity, m/s
$x_s = M_g / (M_g + M_l)$	Static quality, -
$x_e = h_g M_g / (h_g M_g + h_l M_l)$	Equilibrium quality, -
$x_f = W_g / (W_g + W_l)$	Flow quality, -
$J_m = W_m / \rho_m$	Volumetric mixture flow, m^3/s
$J_m = A(j_g + j_l) = J_g + J_l = A\, j_m$	Volumetric mixture flow, m^3/s

Using definitions for the volumetric flow rate and superficial velocity the equation can be written for the flow rates through the junctions with a definite flow area and then the expression used in the code is defined as

$$J_g / \alpha = C_o J_m + A V_{gj} \tag{3.7}$$

From this expression the local void fraction can be derived giving an expression, which is used in the code in the process solving gas and liquid mass flow rates

$$\alpha = \frac{J_g}{C_o J_m + A V_{gj}} \tag{3.8}$$

The velocity difference between phases can be derived using the superficial mixture velocity and drift flux model parameters into the form

$$\Delta u = u_g - u_l = \frac{(C_o - 1) j_m + V_{gj}}{(1 - \alpha)} \tag{3.9}$$

The basic variables in the solution are:

1. Pressure, p
2. Volumetric flow rate, J_m
3. Liquid and gas mass flow rate, W_l, W_g
4. Liquid and gas mass, M_l, M_g
5. Liquid and gas enthalpy, h_l, h_g
6. Concentration noncondensables, C_N.

In addition to these, many calculated quantities are needed. For thermal hydraulics these are void fraction α, mass transfer Γ, heat flux Q and water level Z.

3.3 Derivation of system pressure equation

The principle has been depicted in Figure 8. The system pressure equation is solved applying the volume conservation principle. The system pressure is adjusted in a way that the coolant fills the available volume. When only one volume is handled, no momentum equation is solved for the system pressure.

In the principle of integral momentum solution, a system pressure, steam density and saturation temperature are only functions of the system pressure in the loop. In this way the effect on the steam density are filtered away and the saturation temperature, affecting the steam generation, does not depend on the local pressure variation. The presumption is that the differences of the pressure and the saturation temperature are reasonable compared to the absolute value. The principle may be described through

$$p_i = p_s + \Delta p_i \tag{3.10}$$

$$\rho_{g,i} = f(p_i, h_{g,i}) \approx f(p_s, h_{g,s}) \tag{3.11}$$

$$\rho_{l,i} = f(p_i, h_{l,i}) \approx f(p_s, h_{l,i}) \tag{3.12}$$

$$T_{s,i} = f(p_i) \approx f(p_s) \tag{3.13}$$

where p_i is local pressure, p_s is system pressure. The local liquid density may be a function of the enthalpy, but the density of the gas varies too much for the superheated gas for keeping the simplified solution stable. The system pressure is attached to the steam dome. All evaporation rates and pressure components of the density depend only on this pressure. It is solved as an integrated quantity for the whole vessel volume.

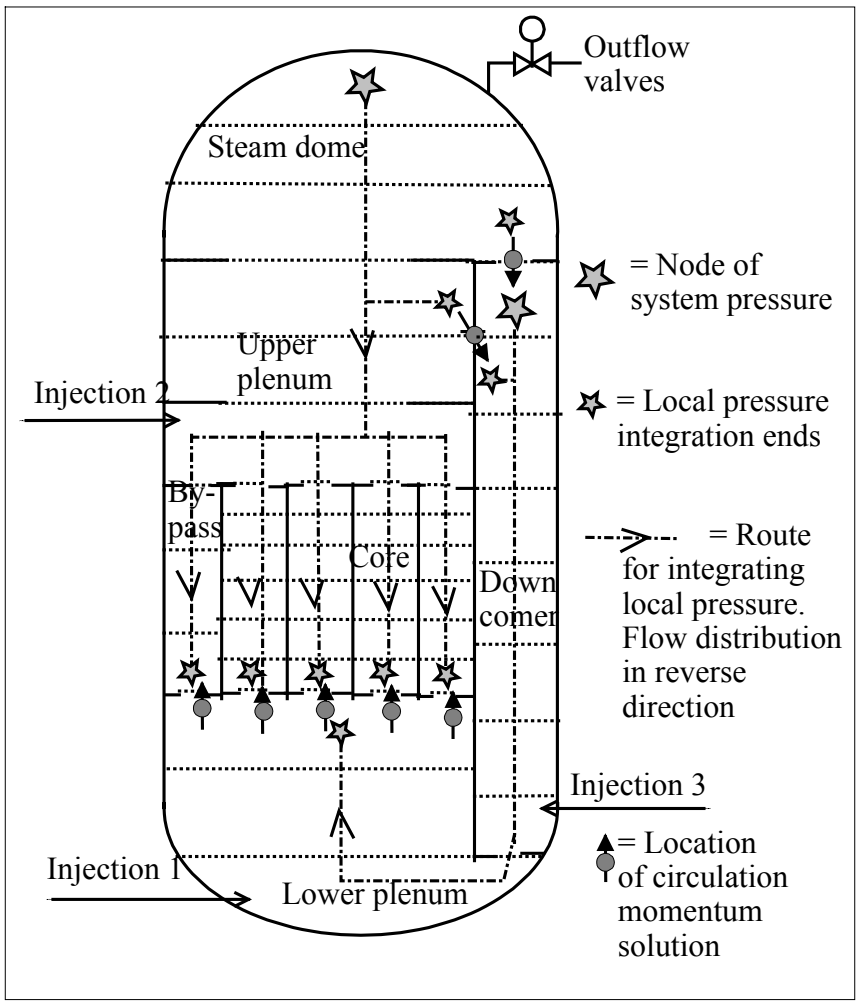

Figure 8. System pressure description and principles of the integral momentum solution in the BWR (RECRIT) application.

Additionally the approach presumes, that also the local pressure distribution is solved. It is needed for calculating the circulation momentum equations in predefined locations. These momentum locations are in the core inlet, one momentum equation into each fuel channel, in the bypass inlet and the recirculation connection from the steam separator into the downcomer. The number of momentum equations needed for the circulation is equal to the number of parallel loops, i.e. degree of freedom in the system.

The multigrid approach has been developed for the solving of the system pressure and circular momentum equations at the same time. In Fig. 8 the basic principle of the multigrid momentum solution has been depicted. The phase mass and mixture momentum equations are solved simultaneously, and then the one solution gives the system pressure in two different regimes and mixture mass flow in the branches between mixture system pressure nodes.

The gas and liquid mass conservations can be written using the volumetric gas flow. The time and spatial derivative are split into two parts giving

$$A\alpha\frac{\partial\rho_g}{\partial t}+A\rho_g\frac{\partial\alpha}{\partial t}+\rho_g\frac{\partial J_g}{\partial z}+J_g\frac{\partial\rho_g}{\partial z}=A\gamma+As_g \tag{3.14}$$

$$A(1-\alpha)\frac{\partial\rho_l}{\partial t}+A\rho_l\frac{\partial(1-\alpha)}{\partial t}+\rho_l\frac{\partial J_l}{\partial z}+J_l\frac{\partial\rho_l}{\partial z}=-A\gamma+As_l \tag{3.15}$$

The derivative of the density is converted into the derivative of pressure through

$$\frac{\partial\rho_g}{\partial t}=\frac{\partial p}{\partial t}\frac{\partial\rho_g}{\partial p}\bigg|_{h_g}+\frac{\partial h_g}{\partial t}\frac{\partial\rho_g}{\partial h_g}\bigg|_{p}\approx\frac{\partial p}{\partial t}\frac{\partial\rho_g}{\partial p}\bigg|_{h_g} \tag{3.16}$$

$$\frac{\partial\rho_l}{\partial t}=\frac{\partial p}{\partial t}\frac{\partial\rho_l}{\partial p}\bigg|_{h_l}+\frac{\partial h_l}{\partial t}\frac{\partial\rho_l}{\partial h_l}\bigg|_{p}\approx\frac{\partial p}{\partial t}\frac{\partial\rho_l}{\partial p}\bigg|_{h_l} \tag{3.17}$$

The partial derivative with respect to the enthalpy is dropped from (3.16) and (3.17) because the enthalpies are solved later than pressures and the effect of the enthalpy on density is considered as a slow changing effect due to large inertia related to the node mass. The resulting equation is expressed through

$$\frac{A\alpha}{\rho_g}\frac{\partial\rho_g}{\partial p}\frac{\partial p}{\partial t}+\frac{J_g}{\rho_g}\frac{\partial\rho_g}{\partial z}+\frac{\partial J_g}{\partial z}=\frac{A}{\rho_g}\gamma+\frac{A}{\rho_g}s_g \tag{3.18}$$

$$\frac{A(1-\alpha)}{\rho_l}\frac{\partial \rho_l}{\partial p}\frac{\partial p}{\partial t}+\frac{J_l}{\rho_l}\frac{\partial \rho_l}{\partial z}+\frac{\partial J_l}{\partial z}=\frac{A}{\rho_l}\gamma+\frac{A}{\rho_l}s_l \tag{3.19}$$

The discretized equation is integrated over the node length and when the nodal mass transfer and mass source terms are derived through

$$\Gamma_i = V_i\ \gamma_i ,\quad S_{l,i}=V_i\ s_{l,i}=\sum_{is} S_{l,is}\ ,\ S_{g,i}=V_i\ s_{g,i}=\sum_{is} S_{g,is} \tag{3.20}$$

$$S_{l,o}=V_i\ s_{l,o}=\sum_{il} S_{l,il}\ ,\quad S_{g,o}=V_i\ s_{g,o}=\sum_{il} S_{g,il} \tag{3.21}$$

the discretized gas and liquid mass conservation equation writes

$$\begin{aligned}&\frac{V_i\alpha_i}{\Delta t\,\rho_g}\left(\frac{\partial \rho_g}{\partial p}\right)_i\left(p_i^{n+1}-p_i^{n}\right)-\sum_{jx} J_{g,j}-\sum_{jx}\frac{<J_{g,j},0>}{\rho_g}\left(\rho_{g,ix}^{n}-\rho_{g,i}^{n}\right)\\&=\frac{\Gamma_i^{n+1}}{\rho_{g,i}}+\frac{S_{g,i}^{n+1}}{\rho_{g,i}}-\frac{S_{g,o}^{n+1}}{\rho_{g,i}}\end{aligned} \tag{3.22}$$

$$\begin{aligned}&\frac{V_i(1-\alpha_i)}{\Delta t\,\rho_l}\left(\frac{\partial \rho_l}{\partial p}\right)_i\left(p_i^{n+1}-p_i^{n}\right)-\sum_{jx} J_{l,j}-\sum_{jx}\frac{<J_{l,j},0>}{\rho_l}\left(\rho_{l,ix}^{n}-\rho_{l,i}^{n}\right)\\&=-\frac{\Gamma_i^{n+1}}{\rho_{l,i}}+\frac{S_{l,i}^{n+1}}{\rho_{l,i}}-\frac{S_{l,o}^{n+1}}{\rho_{l,i}}\end{aligned} \tag{3.23}$$

The steam generation is approximated for the new pressure and new wall temperature through

$$\Gamma_i^{n+1}=\Gamma_i+\frac{\partial \Gamma_i}{\partial T_s}^{n}\left(\frac{\partial T_s}{\partial p}\right)\left(p_i^{n+1}-p_i^{n}\right)+\frac{\partial \Gamma_i}{\partial T_w}^{n}\left(T_w^{n+1}-T_w^{n}\right) \tag{3.24}$$

A corresponding semi-implicit treatment is needed also for outflow terms

$$S_{g,o}^{n+1}=S_{g,o}^{n}+\left(\frac{\partial S_{g,o}}{\partial p}\right)^{n}\left(p_i^{n+1}-p_i^{n}\right)\cong S_{g,o}^{n}+\left(\frac{S_{g,o}}{p}\right)^{n}\left(p_i^{n+1}-p_i^{n}\right) \tag{3.25}$$

$$S_{l,o}^{n+1}=S_{l,o}^{n}+\left(\frac{\partial S_{l,o}}{\partial p}\right)^{n}\left(p_i^{n+1}-p_i^{n}\right)\cong S_{l,o}^{n}+\left(\frac{S_{l,o}}{p}\right)^{n}\left(p_i^{n+1}-p_i^{n}\right) \tag{3.26}$$

By taking into account the semi-implicit approaches and by rearranging the terms in equations, the final formula for the gas and liquid is obtained as

$$\begin{aligned}&(\frac{V_i \alpha_i}{\Delta t \rho_g}(\frac{\partial \rho_g}{\partial p})_i - \frac{1}{\rho_{g,i}}(\frac{\partial \Gamma_i}{\partial p}) + \frac{1}{\rho_{g,i}}(\frac{S_{g,o}}{p^n}))(p_i^{n+1} - p_i^n) = \\ &-\sum_{jx}\frac{< J_{g,j}, 0 >}{\rho_g}(\rho_{g,ix}^n - \rho_{g,i}^n) - \sum_{jx} J_{g,j} + \frac{\Gamma_i^n}{\rho_{g,i}} + \frac{S_{g,i}^n}{\rho_{g,i}} - \frac{S_{g,o}^n}{\rho_{g,i}}\end{aligned} \tag{3.27}$$

$$\begin{aligned}&(\frac{V_i (1-\alpha_i)}{\Delta t \rho_l}(\frac{\partial \rho_l}{\partial p})_i + \frac{1}{\rho_{l,i}}(\frac{\partial \Gamma_i}{\partial p}) + \frac{1}{\rho_{l,i}}(\frac{S_{l,o}}{p}))(p_i^{n+1} - p_i^n) = \\ &-\sum_{jx}\frac{< J_{l,j}, 0 >}{\rho_l}(\rho_{l,ix}^n - \rho_{l,i}^n) - \sum_{jx} J_{l,j}, 0 + \frac{\Gamma_i^n}{\rho_{l,i}} + \frac{S_{l,i}^n}{\rho_{l,i}} - \frac{S_{l,o}^n}{\rho_{l,i}}\end{aligned} \tag{3.28}$$

The numerical solution is based on a multistage procedure for the pressure, void fraction and enthalpy, the error in the mass balance can not be avoided. The sources are the truncation error, and it is defined through

$$D_i = \frac{M_{g,i}}{\rho_{g,i}} + \frac{M_{l,i}}{\rho_{l,i}} - V_i \tag{3.29}$$

A relaxation parameter of 0.3 is used for the term. The mass conservation equations may be written by defining the collective terms T and U as follows

$$B_{g,i} p_i^{n+1} = B_{g,i} p_i^n + \sum_{jx} J_{g,j}^{n+1} + C_{g,i}^n$$

$$B_{l,i}\, p_i^{n+1} = B_{l,i}\, p_i^n + \sum_{jx} J_{l,j}^{n+1} + C_{l,i}^n \tag{3.30}$$

which give by summing the discretized mixture mass equation as

$$(B_{g,i} + B_{l,i})\, p_i^{n+1} = (B_{g,i} + B_{l,i})\, p_i^n + \sum_{jx} J_{m,j}^{n+1} + (C_{g,i} + C_{l,i}) + D_i / \Delta t \tag{3.31}$$

or

$$B_{m,i}\, p_i^{n+1} = B_{m,i}\, p_i^n + \sum_{jx} J_{m,j}^{n+1} + C_{m,i} + E_{m,i} \tag{3.32}$$

with following values for the coefficients

$$B_{m,i} = \frac{V_i}{\Delta t}\left(\frac{\alpha_i}{\rho_g}(\frac{\partial \rho_g}{\partial p})_i + \frac{(1-\alpha_i)}{\rho_l}(\frac{\partial \rho_l}{\partial p})_i\right) - \frac{\rho_{l,i}-\rho_{g,i}}{\rho_{g,i}\,\rho_{l,i}}(\frac{\partial \Gamma_i}{\partial p}) + \frac{1}{\rho_{g,i}}(\frac{S_{g,o}}{p^n}) \tag{3.33}$$

$$\begin{aligned} C_{m,i} = &-\sum_{jx}\frac{<J_{g,j},0>}{\rho_g}(\rho^n_{g,ix}-\rho^n_{g,i}) - \sum_{jx}\frac{<J_{l,j},0>}{\rho_l}(\rho^n_{l,ix}-\rho^n_{l,i}) \\ &+\frac{S^n_{l,i}}{\rho_{l,i}} - \frac{S^n_{l,o}}{\rho_{l,i}} + \frac{\Gamma^n_i}{\rho_{g,i}} + \frac{S^n_{g,i}}{\rho_{g,i}} - \frac{S^n_{g,o}}{\rho_{g,i}} \end{aligned} \tag{3.34}$$

$$D_{m,i} = \left(\frac{M_{g,i}}{\rho_{g,i}} + \frac{M_{l,i}}{\rho_{l,i}} - V\right)\frac{1}{\Delta t} \tag{3.35}$$

The momentum equations are discretized starting from the primitive form of the momentum equations. If the phase velocity is replaced by the volumetric flow rate, the gas momentum equation may be formulated giving

$$\begin{aligned} &(\frac{\Delta z_j \rho_{g,j}}{\Delta t A_j} - \sum_{jx}\frac{\rho_{g,j}\Delta u_{g,j}}{A_j} + \frac{0.5\rho_g X_{k,j}\alpha_j\left|u_{g,j}\right|}{A_j})J^{n+1}_{g,j} = (\frac{\Delta z_j \rho_{g,j}}{\Delta t A_j})J^n_{g,j} \\ &+\alpha_j(p^{n+1}_{i1} + \Delta p_{i1} + \frac{\partial \Delta p_{i1}}{\partial J_{g,j}}(J^{n+1}_{g,j} - J^n_{g,j}) - p^{n+1}_{i2} - \Delta p_{i2} - \frac{\partial \Delta p_{21}}{\partial J_{g,j}}(J^{n+1}_{g,j} - J^n_{g,j})) \\ &+\alpha_j \Delta p_{e,j} - \alpha_j \Delta z_j \rho_{g,j}\, g\cos\theta_j - F_{ij} \end{aligned} \tag{3.36}$$

and the liquid momentum equation

$$\begin{aligned} &(\frac{\Delta z_j \rho_{l,j}}{\Delta t A_j} - \sum_{jx}\frac{\rho_{l,j}\Delta u_{l,j}}{A_j} + \frac{0.5\rho_l X_{k,j}(1-\alpha_j)\left|u_{l,j}\right|}{A_j})J^{n+1}_{l,j} = (\frac{\Delta z_j \rho_{l,j}}{\Delta t A_j})J^n_{l,j} \\ &+(1-\alpha_j)(p^{n+1}_{i1} + \Delta p_{i1} + \frac{\partial \Delta p_{i1}}{\partial J_{g,j}}(J^{n+1}_{l,j} - J^n_{l,j}) - p^{n+1}_{i2} - \Delta p_{i2} - \frac{\partial \Delta p_{21}}{\partial J_{g,j}}(J^{n+1}_{l,j} - J^n_{l,j})) \\ &+(1-\alpha_j)\Delta p_{e,j} - (1-\alpha_j)\Delta z_j \rho_{l,j}\, g\cos\theta_j - F_{ij} \end{aligned} \tag{3.37}$$

Here the derivative of the dynamic pressure with respect to the volumetric flow rate change is expressed through

$$\frac{\partial p}{\partial J} = \sum_{ip1}^{ip2} = 0.5\times(\frac{\Delta z\, f_j}{D_e} + X_j)(\alpha\rho_g\left|u_g\right| + (1-\alpha)\rho_l\left|u_l\right|)\frac{1}{A_j} \tag{3.38}$$

The integration node for the momentum equation composes halves of the volumes connected by the junction. In F_{ij} denotes the interphasial momentum. If both equations are solved at the same time together, the interphasial friction would be the most difficult term to formulate. The equations may be written for the gas flow in a shortened form as

$$(E_{g,j} + G_{g,j} + F_{g,j})\, J_{g,j}^{n+1} = (E_{g,j} + G_{g,j}) J_{g,j}^{n} + \alpha_j^n (p_{i1}^{n+1} - p_{i2}^{n+1}) + H_{g,j} - F_{ij} \tag{3.39}$$

$$(E_{l,j} + G_{l,j} + F_{l,j})\, J_{l,j}^{n+1} = (E_{l,j} + G_{l,j}) J_{l,j}^{n} + (1-\alpha_j^n)(p_{i1}^{n+1} - p_{i2}^{n+1}) + H_{l,j} + F_{ij} \tag{3.40}$$

The summation gives the final expression for the mixture momentum equation

$$\begin{aligned}(E_{g,j} + E_{l,j} + G_{g,j} + G_{l,j} + F_{g,j} + F_{l,j})\, J_{m,j}^{n+1} = (E_{g,j} + E_{l,j} + G_{g,j} + G_{l,j})\, J_{m,j}^{n} \\ + (p_{i1}^{n+1} - p_{i2}^{n+1}) + (H_{g,j} + H_{l,j})\end{aligned} \tag{3.41}$$

or as written in the mixture form as

$$(E_{m,j} + G_{m,j} + F_{m,j})\, J_{m,j}^{n+1} = (E_{m,j} + G_{m,j})\, J_{m,j}^{n} + (p_{i1}^{n+1} - p_{i2}^{n+1}) + H_{m,j} \tag{3.42}$$

The different coefficients may be expressed through

$$E_{m,j} = \frac{1}{\Delta t} \sum_{ip1}^{ip2} \left(\frac{\Delta z_j}{A_j} \left(\alpha_j \rho_{g,i} + (1-\alpha_j) \rho_{l,i} \right) \right) \tag{3.43}$$

$$G_{m,j} = -\frac{\partial \Delta p_{i1}}{\partial J_{g,j}} + \frac{\partial \Delta p_{21}}{\partial J_{g,j}} \tag{3.44}$$

$$F_{m,j} = \frac{0.5 \rho_g X_{k,j} \alpha_j \left| u_{g,j} \right|}{A_j} + \frac{0.5 \rho_l X_{k,j} (1-\alpha_j) \left| u_{l,j} \right|}{A_j} \tag{3.45}$$

$$H_{m,j} = \Delta p_{e,j} - \left(\alpha_j \rho_{g,j} + (1-\alpha_j) \rho_{l,j} \right) \Delta z_j \, g \cos\theta_j + \Delta p_{i1} - \Delta p_{i2} \tag{3.46}$$

Now the momentum equation has a form, that it can be inserted into the mass conservation equation.

$$B_{m,i}\, p_i^{n+1} - \sum_{jx}\left[\frac{1}{(E_{m,j}+G_{m,j}+F_{m,j})}(p_{ix}^{n+1} - p_i^{n+1})\right] =$$
$$B_{m,i}\, p_i^{n} + \sum_{jx}\left[\frac{G_{m,j}}{(E_{m,j}+G_{m,j}+F_{m,j})} J_{m,j}^{n} + \frac{1}{(E_{m,j}+G_{m,j}+F_{m,j})} H_{m,j}\right] \qquad (3.47)$$
$$+\ C_{m,i} + E_i/\Delta t$$

The solution for a two node system may be written in the compact form

$$\begin{aligned} C_1\, p_1^{n+1} + U_1 p_2^{n+1} &= R_1^n \\ L_2 p_1^{n+1} + C_2 p_2^{n+1} &= R_2^n \end{aligned} \qquad (3.48)$$

This gives the pressures as a solution

$$\begin{aligned} p_2^{n+1} &= (R_2^n - R_1^n \frac{L_2}{C_1})/(C_2^n - U_1^n \frac{L_2}{C_1}) \\ p_1^{n+1} &= (R_1^n - U_1 p_2^{n+1})/C_1 \end{aligned} \qquad (3.49)$$

After updating the system pressure the flow rate in all junctions between the system pressure nodes is solved directly from

$$J_{m,j}^{n+1} = \frac{(E_{m,j}+G_{m,j})}{(E_{m,j}+G_{m,j}+F_{m,j})} J_{m,j}^{n} + \frac{(p_{i1}^{n+1} - p_{i2}^{n+1}) + H_{m,j}}{(E_{m,j}+G_{m,j}+F_{m,j})} \qquad (3.50)$$

After solving the new pressure the boiling and leakage terms have to be updated by using following equations before final integration of the mass balance.

$$\Gamma_i^{n+1} = \Gamma_i + \frac{\partial \Gamma_i}{\partial T_s}^{n}\left(\frac{\partial T_s}{\partial p}\right)\left(p_S^{n+1} - p_S^{n}\right) \qquad (3.51)$$

$$W_{lo}^{n+1} = W_{lo}^{n} + (\frac{dW_{lo}}{dp})(\ {p_S}^{n+1} - {p_S}^{n}\ ) \qquad (3.52)$$

$$W_{go}^{n+1} = W_{go}^{n} + (\frac{dW_{go}}{dp})(\ {p_S}^{n+1} - {p_S}^{n}\ ) \qquad (3.53)$$

The system pressure is solved in the module PRESSU.

3.4 Derivation of local pressure distribution

After solving the system pressure, the pressure distribution is solved inside the system. The wall friction over a junction of integration volumes over the length $\Delta z = 0.5(\Delta z_{i1} + \Delta z_{i2})$, is in a formula for the pressure loss for the mixture flow.

$$\Delta p = p_{i-1} - p_i = 1/2\left(\frac{\Delta z\, f_j}{D_e} + X_j\right)\left(\alpha\rho_g u_g |u_g| + (1-\alpha)\rho_l u_l |u_l|\right) + A\rho_l g \cos\theta \qquad (3.54)$$

The friction coefficient X includes the singular pressure drops. The term *f* accounts for the wall shear.

The integration of the pressure distribution is started from the system pressure node and it marches in the reverse order of junction indices. Marching is stopped at the momentum solution junctions.

The local pressure distribution is solved in the module PREDIS.

3.5 Derivation of circulation momentum

The circulation momentum is solved after finding the pressured distribution. The system pressure node is located uppermost in the steam dome. The momentum solution points are located in the inlet into each core channel, inlet into the bypass system and at the location of the back circulation from the steam separator to the downcomer. For system with parallel circulation paths the number of momentum equations is equal to the number of independent circulation loops. As a consequence the pressure difference over the momentun junctions is defined through

$$\Delta p_{mom} = p_{i1} - p_{i2} \qquad (3.55)$$

For this pressure difference the flow acceleration may be solved for the volumetric flow which gives the following value

$$J_{mom}^{n+1} = J_{mom}^{n} + \int_{loop} \frac{\Delta p_{mom}}{\Delta z_{mom}\rho_m}\Delta t \qquad (3.56)$$

In the equation Δp_{mom} means the pressure difference over the momentum junction and Δz_{loop} is an appropriate length to be used for the momentum equation. The length is not the whole circuit length. For a simple U-tube it could be the length of the water column. A practical measure used in GENFLO is $\Delta z_{loop} = 2$ m.

The circulation rate through the integral momentum junctions is solved in the module CIRCUL.

3.6 Solution of local volumetric flow distribution

After the integral loop momentum is solved, the local mixture flow is solved from the steady state mixture mass conservation equation for the node

$$J_{m,j} = \sum_{to\ i}^{jx} J_{m,jx} + \Gamma_i\left(\frac{1}{\rho_{g,i}} - \frac{1}{\rho_{l,i}}\right) + \frac{S_{g,i}}{\rho_{g,i}} + \frac{S_{l,i}}{\rho_{l,i}} + \sum_{to\ i}^{jx} W_{l,j}\left(\frac{1}{\rho_{l,ix}} - \frac{1}{\rho_{l,i}}\right) + \sum_{to\ i}^{jx} W_{g,j}\left(\frac{1}{\rho_{g,ix}} - \frac{1}{\rho_{g,i}}\right) \tag{3.57}$$

For the discretization the indexing order is important. For calculating flow in junction j, the other junctions jx connected into the node i have a lower index value. The node ix means the node on the other side of the junction j. The distribution of the local volumetric flow and definition of the phase separation is solved in the module FLOVOL.

3.7 Solution of phase separation and junction mass flow rates

The solution of the combined mixture mass and momentum equation gives the pressure and volumetric flow distributions in the system. In the next step the phase separation is solved, giving phase velocities. This step can no longer be done on the velocity basis, because new densities have been defined in the pressure integration and the mass flow rate, product of volumetric flow rate and density gives liquid flow rate. The drift flux formula can be used for the derivation of the gas mass flow rate as

$$W_{g,j} = A_j \rho_{g,j} \alpha_j (C_0 j_m + V_{gj}) \tag{3.58}$$

For the integration the equation is discretized giving

$$W_{g,j}^{n+1} = \rho_{g,j}^{n} J_{g,j}^{n+1} = \rho_{g,j}^{n} \alpha_j^{n+1} (C_0 J_{m,j}^{n+1} + A_j V_{gj}^{n}) \tag{3.59}$$

Finding a guess for the new void fraction is necessary for the stability. The solution would be stable by using the old void fraction. The flow direction defines, from which node the void fraction is picked for the junction, as follows

$$\alpha_j^{n+1} = \alpha_{i1}^n \quad \text{if} \qquad u_{g,j} > 0 \tag{3.60}$$

The guess for the void fraction is solved as an intermediate parameter. The expression may be formulated from the gas mass conservation equation as

$$\alpha_i^{n+1} \rho_{g,i}^{n+1} V_i = \alpha_i^n \rho_{g,i}^{n+1} V_i + \sum_{to\, i} < J_{m,j}^{n+1}, 0 > \alpha_j^{n+1} V + \max(S_{g,i}^{n+1}, 0) \Delta t \tag{3.61}$$

The notation <a,0> means that only flows coming into the node are considered. The Equation (3.61) written for all nodes composes a set of algebraic equations, where the new time step void fraction is needed for the neighbouring node, also. The solution would require matrix inversion. This is not used. The system creates indexing in such a way, that by looping junction indexes in the ascending direction follows the normal flow direction: from bottom of the core to top over all rings, the bypass from bottom to top, upper plenum from bottom to top, steam separator from bottom to top, lower plenum from top to bottom, downcomer from bottom to top and finally steam dome from bottom to top. At first the junctions are looped in the ascending order and after this another loop in the inverse direction. The solution is an application of the Gauss-Seidel iteration by a bi-directional sweep.

The guessed void fraction is not used as a mass conservation parameter, however. Instead the gas mass flow is solved from the Equation (3.62). The liquid flow rate may be calculated from the fact that the mixture flow is the sum of liquid and vapour mass flows through equation

$$W_{l,j}^{n+1} = (J_{m,j}^{n+1} - W_{g,j}^{n+1} / \rho_{g,j}^{n+1}) \rho_{l,j}^{n+1} \tag{3.62}$$

The selected numerical solution leads easily to a situation where steam or liquid mass is negative. For this type of situation it is defined

$$W_{l,j} = 0.0 \quad \text{if} \quad M_{l,i} < 0.0 \tag{3.63}$$

After using the limitation the steam mass flow is again recalculated from the equation

$$W_{g,j}^{n+1} = (J_{m,j}^{n+1} - W_{l,j}^{n+1} / \rho_{l,j}^{n+1}) \rho_{g,j}^{n+1} \tag{3.64}$$

The phase mass flow rates are defined in the module FLOMAS.

The mass conservation equations are finally updated in the module ENEBAL using an explicit integration for conserving the mass balance

$$M_{g,i}^{n+1} = M_{g,i}^{n} + (\sum_{to\ i}^{j} W_{g,j}^{n+1} + S_{g,i}^{n+1} - S_{g,o}^{n+1} + \Gamma_i^{n+1})\Delta t \tag{3.65}$$

$$M_{l,i}^{n+1} = M_{l,i}^{n} + (\sum_{to\ i}^{j} W_{l,j}^{n+1} + S_{l,i}^{n+1} - S_{l,o}^{n+1} - \Gamma_i^{n+1})\Delta t \tag{3.66}$$

3.8 Solution of wall heat transfer and interphasial heat transfer

The basic quantities for the heat flux definition are depicted in Figure 9.

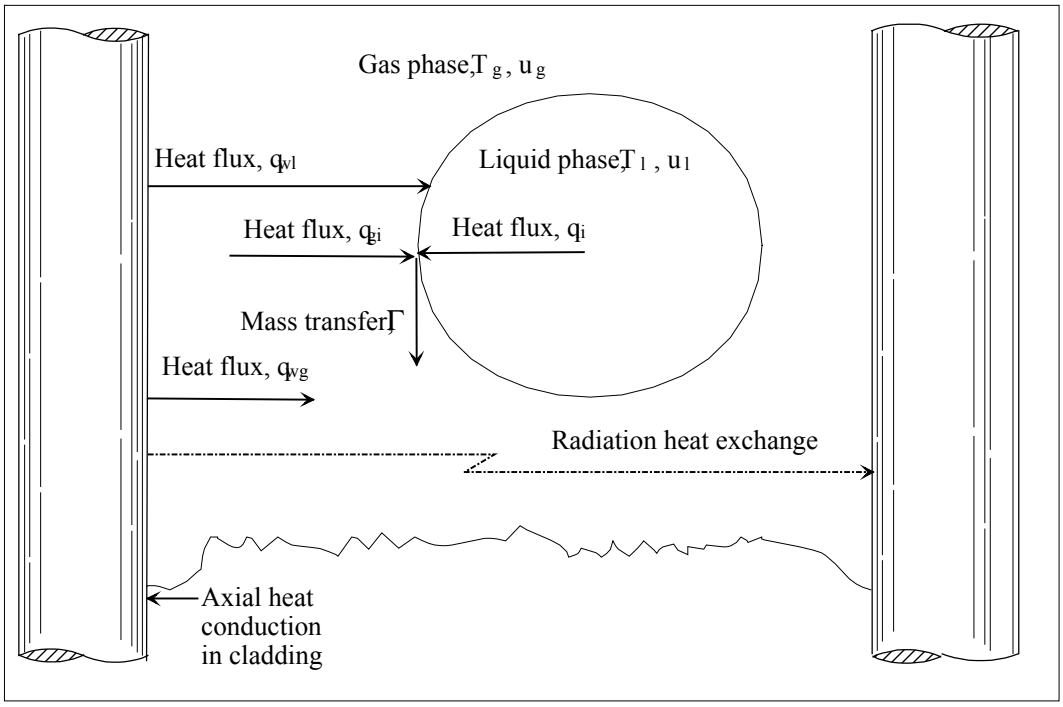

Figure 9. Basic definitions for the energy integration of two-phase equations.

The heat flux rates on the right hand sides are defined separately for the heat transfer from wall to liquid, wall to vapour and between phases. The heat flux rate here means a volumetric rate and it is related to the surface heat flux by

$$q_{wg}''' = q_{wg}'' \frac{4}{D_e} = q_{wg}'' \frac{P_{wg}}{A} \tag{3.67}$$

$$q_{wl}''' = q_{wl}'' \frac{4}{D_e} = q_{wl}'' \frac{P_{wl}}{A} \tag{3.68}$$

The heat transfer coefficient is typically defined via the transfer correlations for convective heat transfer

$$q''_{wg} = h_{wg}(T_w - T_g) \tag{3.69}$$

$$q''_{wl} = h_{wl}(T_w - T_l) \tag{3.70}$$

For the boiling heat transfer typically applies that (n = 1.0 ... 3) in equation

$$q''_{wb} = h_{wb}(T_w - T_s)^n \tag{3.71}$$

The net mass transfer due to the wall heat transfer is formulated through

$$\gamma''_w = \frac{q''_{wb} + F_b q''_{wl}}{h_{lg}} \tag{3.72}$$

where F_b is the evaporation fraction for the convection heat flux and it is defined as a function of the liquid subcooling.

The interphasial flashing heat transfer is defined in the form

$$q'''_{li} = h_{li,f}\, max(T_l - T_s, 0.0) \tag{3.73}$$

The interfacial condensation heat transfer is defined in the form

$$q'''_{li} = -h_{li,c}\, max(T_s - T_l, 0.0) \tag{3.74}$$

The heat from the superheated gas to the liquid surface is defined in the form

$$q'''_{gi} = h_{gi}\, max(T_g - T_s, 0.0) \tag{3.75}$$

The net mass transfer due to the interphasial heat transfer is formulated in the following way

$$\gamma'''_i = \frac{q'''_{li,f} - q'''_{li,c} + q'''_{gi}}{h_{lg}} \tag{3.76}$$

The heat transfer equations are solved in the module REFLOD.

3.9 Solution of enthalpy equation

The enthalpy is related to the internal energy through the relationship

$$h=e+\frac{p}{\rho} \tag{3.77}$$

Integration of the gas energy equation has been realized by multiplying the gas mass conservation equation by gas enthalpy and by subtracting the equation from conservation type of equation. Similarly the liquid conservation equation is multiplied by liquid enthalpy and subtracted from the liquid enthalpy equation. The new formulas are the primitive forms of equations. The primitive form does not guarantee full energy conservation, but instead it offers a stable solution for the conservation equations.

Gas enthalpy equation in the primitive form is written

$$A\alpha\rho_g \frac{\partial(h_g)}{\partial t}+A\alpha\rho_g u_g \frac{\partial(h_g)}{\partial z}=Aq'''_{wg}+Aq'''_{lg}+A\gamma(h_{gs}-h_g)+As_g(h_{S,g}-h_g) \tag{3.78}$$

Liquid enthalpy equation in the primitive form is written through

$$A(1-\alpha)\rho_l \frac{\partial(h_l)}{\partial t}+A(1-\alpha)\rho_l u_l \frac{\partial(h_l)}{\partial z}=Aq'''_{wl}+Aq''''_{ll}-A\gamma(h_{sl}-h_l)+As_l(h_{S,l}-h_l) \tag{3.79}$$

The numerical solution is written for this equation by replacing the time derivative by the timestep and space derivative by the node length. The convection term is discretised by the donor cell principle. By looping the indexes in the ascending direction, the normal flow direction is followed for most of the flow path. The integration realises the Gauss-Seidel iteration principle. The enthalpy equations may be solved by a reasonable accuracy in a one loop over indexes for the convective terms.

The discretized presentation of the gas enthalpy equation for the Equation (3.78) is written in the following way

$$\begin{aligned} &M^n_{g,i}(h^{n+1}_{g,j}-h^n_{g,j})+\sum_{>i}<W^{n+1}_{g,j},0>(h^{n+1}_{g,x}-h^n_{g,ix})\Delta t=+Q^{n+1}_{wg}\Delta t+Q^{n+1}_{ig}\Delta t \\ &+max\left(\Gamma^{n+1}_i,0\right)(h^{n+1}_{s,i}-h^n_{g,j})\Delta t+S^{n+1}_{g,in}(h_{g,S,i}-h^{n+1}_{g,i})\Delta t \end{aligned} \tag{3.80}$$

The discretized presentation of the liquid enthalpy equation for the Equation (3.79) is written as follows

$$M_{l,i}^{n}(h_{l,j}^{n+1}-h_{l,j}^{n})+\sum_{to\,i}<W_{l,j}^{n+1},0>(h_{l,i}^{n+1}-h_{l,ix}^{n})\Delta t=Q_{wl}^{n+1}\Delta t+Q_{il}^{n+1}\Delta t$$
$$+max\left(-\Gamma_{i}^{n+1},0\right)(h_{ls,i}^{n+1}-h_{l,j}^{n})\Delta t+S_{l,in}^{n+1}(h_{l,S,i}-h_{l,i}^{n+1})\Delta t \qquad (3.81)$$

Also this equation is solved by the same principles as the equation for the gas enthalpy conservation.

The brackets <W,0> mean, that only the flow rates coming into the node i are considered. The index ix for the enthalpy means the donoring node.

The heating flux for coolant needs estimation for the new timestep by taking into account the enthalpy change during the timestep. This kind of source term linearization makes possible the integration by longer timesteps than could be possible by using an explicit integration. The estimates or gas and liquid heating are

$$Q_{g,i}^{n+1}=Q_{g,i}^{n}+\frac{1}{c_{pg}}\frac{\partial Q_{g,i}}{\partial T_{g}}^{n}\left(h_{g,i}^{n+1}-h_{g,i}^{n}\right) \qquad (3.82)$$

$$Q_{l,i}^{n+1}=Q_{l,i}^{n}+\frac{1}{c_{pl}}\frac{\partial Q_{l,i}}{\partial T_{g}}^{n}\left(h_{l,i}^{n+1}-h_{l,i}^{n}\right) \qquad (3.83)$$

The Equations (3.80) and (3.81) written for all nodes in the system define a set of algebraic equations, from which the new enthalpies may be solved. Iteration is needed, because the enthalpies of neighbouring nodes are assumed as new timestep enthalpies. No matrix inversions or full iteration have been performed, however. The calculation is done in a single sweep in the order of indexing . Thus the in-flowing enthalpy comes from the same timestep.

The equations for the enthalpies and integration of mass conservation is solved in the module ENEBAL.

3.10 Solution of noncondensables in gas

The integration for the dissolved concentration of noncondensables may be done with a simple method based on the donor cell discretization of the equation

$$(M_{g,i}^{n} + \sum_{to\,i} < W_{g,j}^{n+1}, 0 > \Delta t\,) C_{N,i}^{n+1} - \sum_{to\,i} < W_{g,j}^{n+1}, 0 > \Delta t\, C_{N,ix}^{n+1} =$$
$$- \Gamma_i^{n+1} C_{N,i}^{n+1} \Delta t + S_{g,in}^{n+1} C_{N,S,i} \Delta t \tag{3.84}$$

Also these equations written for all nodes define a set of algebraic equations, which is solved in a single sweep by looping over all indexes. The equations of the noncondensable gas are integrated in the module ENEBAL.

3.11 Steam tables for conservation equations

The material properties depend on pressure and enthalpy:

$$\begin{aligned} \rho_l &= f\ (p, h_l) \\ \rho_g &= f\ (p, h_g) \\ h_{ls} &= f\ (p) \\ h_{gs} &= f\ (p) \\ T_s &= f\ (p) \end{aligned} \tag{3.85}$$

The derivatives are needed for pressures and they are defined as a numerical derivation of the material functions. Additional material properties are the heat capacities and conductivities for the liquid and vapour.

4. Constitutive models

4.1 Concept of the heat transfer model

The considered flow modes, single phase liquid or steam, bubble or slug flow, annular or inverted annular flow, dispersed droplet flow and swell level are depicted in the Figure 10. In the heat transfer concept, the corresponding heat transfer modes as well as the rod surface is shared into two sections, wetted wall and dry wall by the quenching front.

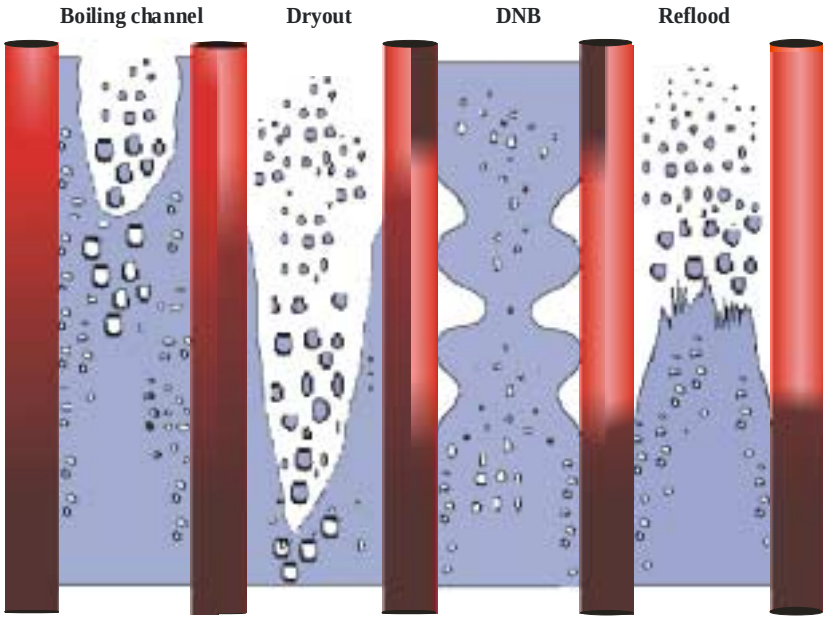

Figure 10. Channel flow modes considered in GENFLO model.

In the wetted part the convection into single-phase liquid and steam and boiling are considered. The heat flux is limited by the critical heat flux correlation of the pool boiling. As long as the liquid is subcooled, a part of the heat is used for the liquid heatup. The liquid continuous part is assumed to end at the quench front.

The heat transfer coefficient decreases across the quenching front by more than two orders of magnitude. The quenching front is a combination of the transient boiling and axial heat conduction in the cladding. The quenching front movement and its cooling effect are calculated by an analytical correlation, where the effective heat transfer in the wetted part and the Leidenfrost temperature are used as fitting parameters.

In the post-dryout regime above the quenching front the heat transfer surface is not wetted and six heat transfer mechanisms are included in the conceptual model: 1.

transition boiling, 2. film boiling, 3. steam heating by convection, 4. interfacial heat transfer between superheated steam to liquid droplets, 5. radiation absorption into droplets and 6. radiation heat exchange between solid structures.

The post-dryout heat transfer and quench front velocity modelling are the most important processes in reflooding analysis. In integral codes the heat transfer package typically includes less heat transfer modes, but the correlations may describe several heat transfer modes by using a single correlation. In the approach of GENFLO the assumption is, that all heat transfer modes exist over the whole post-dryout regime. In addition it is assumed, that the liquid volumetric fraction, the inverse of the void fraction, is the main parameter defining the strength of the heat transfer mode. But in addition to this user dials have been defined for further tuning of different heat transfer modes.

4.2 Wetted wall heat transfer

The wetted wall heat transfer model is based on modelling of the different sections in the boiling curve, depicted in Figure 11.

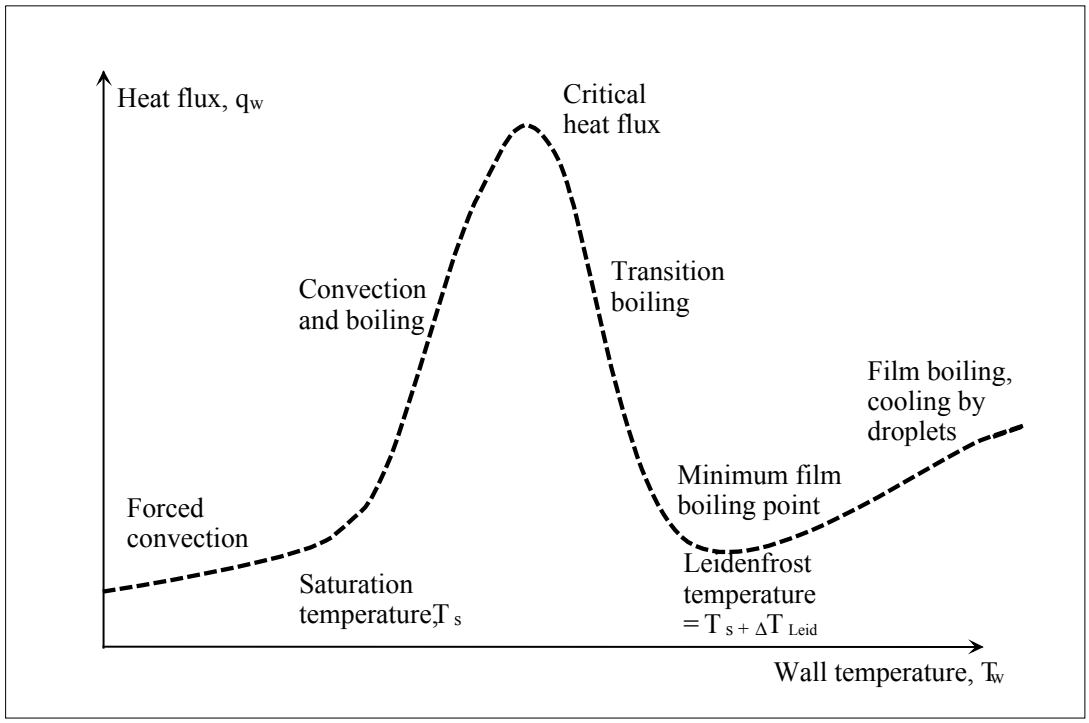

Figure 11. Different sections in the boiling curve.

When the wall temperature is below the saturation temperature, heat transfer takes place by forced convection to sub-cooled liquid. The heat transfer coefficients for the laminar and turbulent convection are defined as

$$h_{cl} = 4.36\, D_h / \mu_l \tag{4.1}$$

if Re < 2000 else Dittus-Boelter correlation is used

$$Re_\ell = \frac{W_l\, D_e}{A \mu_\ell} \tag{4.2}$$

$$h_{lc} = \frac{\lambda_l}{D_e} 0.023 \cdot Re_\ell^{0.8} \cdot Pr_\ell^{0.4} \tag{4.3}$$

For simplicity $Pr_l = 1.0$ is assumed.

For the regime with convection and boiling together a formalism proposed by Chen has been realized. In the formalism a nucleate boiling heat transfer coefficient is defined originally on the basis of pool boiling studies. The boiling heat transfer has a form

$$h_{nb}^{\ *} = 0.00122 \frac{\lambda_l^{0.79} c_{p_l}^{\ 0.45} \rho_l^{0.49} \Delta T^{0.24} \Delta\, p^{0.75}}{\sigma^{0.5} \mu_l^{0.29} h_{lg}^{0.24} \rho_g^{0.24}} \tag{4.4}$$

but it is not practical to be used in this form. The term including Δp needs to be converted. Together with ΔT an estimation may be written as

$$\Delta T^{0.24} \Delta\, p^{0.75} = (T_w - T_s)^{0.24} (p_w - p_s)^{0.75} = (T_w - T_s)^{0.99} \left(\frac{\partial T_s}{\partial p} \right)^{0.75} \approx (T_w - T_s) \left(\frac{\partial T_s}{\partial p} \right)^{0.75} \tag{4.5}$$

By applying this relationship the nucleate boiling heat transfer can be expressed as

$$h_{nb} = h_{nb}^{\ *} \left[\frac{\partial T_s}{\partial p} \right]^{0.75} (T_w - T_s) \tag{4.6}$$

Originally Chen proposed the total heat flux for the wetted wall with convection and boiling written through

$$q_w = h_{nb} \cdot (T_w - T_s) S + h_{cl} \cdot (T_w - T_l) F \tag{4.7}$$

where the coefficient S = nucleation boiling suppression factor (S = 0 … 1) and F = convection amplification (F > 1). The parameters attempt to describe a boiling channel with forced evaporation thought the annular liquid film, when the quality increases along the channel. This type of flow pattern has not been included into the conceptual model- That is why S = 1 and F = 1 have been assumed. Remark that through Equation (4.6) the boiling term includes the wall superheating as a second power in the heat flux. Quite many boiling heat transfer models can be written using this dependency.

The Thom nucleate boiling model is defined through

$$h_{nb} = \frac{10^6}{22.52^2} exp(0.023 \times p_{bar}) \ (T_w - T_s) \tag{4.8}$$

and if this correlation is applied for the wetted wall heat transfer, the expression for the heat flux would be

$$q_w = h_{nb} \cdot (T_w - T_s) + h_{cl} \cdot (T_w - T_l) \tag{4.9}$$

In the Table 2. the heat transfer coefficients for the wetted wall have been compared.

Table 2. Typical heat transfer values by classical heat transfer correlations.

Correlation	Use	h as W/m^2/K or W/m^2/K^2		
		1 bar, 1 m/s	10 bar, 1 m/s	70 bar, 1 m/s
Dittus-Boelter	$q = h_c*(T_w-T_l)$	1035.	5747	9133
Thom NB	$q = h_b*(T_w-T_s)^2$	2017.	2481.	9864.
Chen NB	$q = h_b*(T_w-T_s)^2$	1025.	2845.	8522.
GENFLO NB	$q = h_b*(T_w-T_s)^2$	2025.	2250.	3750.

In GENFLO the convection heat transfer is solved from Equations (4.1) and (4.3). The nucleate boiling heat transfer coefficient has been extrapolated as

$$h_b = 2.5x10^{-4} \cdot p + 2000. \tag{4.10}$$

If the total heat flux in the wetted zone exceeds the critical heat flux, the critical heat flux value has been set. The critical heat flux model of GENFLO is a simplified fit to typical critical heat flux correlations and the expression is written as follows

$$F_x = min(1 - \alpha \times 0.6, 1 - \alpha^2, 1 - x^2) \tag{4.11}$$

$$q_{chf} = (1.0 \times 10^6 + max(0.801 \times p - 4.64 \times 10^{-8} p^2, 0.0) \times F_x \quad (4.12)$$

In Table 3 typical values for known critical heat flux correlations are given. The discrepancy between different models is quite large. That is the reason, why finally an own correlation has been developed.

The Griffith-Zuber pool boiling critical heat flux model is formulated through

$$q_{CHF} = 0.131(1-\alpha)\rho_g h_{fg} \left(\frac{\sigma g(\rho_l - \rho_g)}{\rho_g^2}\right)^{0.25} \quad (4.13)$$

The Biasi flow boiling critical heat flux model is formulated through

$$F = 0.7249 + 0.99 P e^{-0.3P} \quad (4.14)$$

$$H \equiv -1.159 + 1.49 P e^{-0.19P} + \frac{90P}{10 + (10P)^2}$$

$$q_{CHF1} = \frac{1.883 \times 10^7}{(100D)^N (G/10)^{0.167}} \left(\frac{F}{(G/10)^{0.167}} - x\right)$$

$$q_{CHF2} = \frac{3.78 \times 10^7 H(1-x)}{(100D)^N (G/10)^{0.6}}$$

$$q_{CHF} = max(q_{CHF1}, q_{CHF2})$$

with P = MPa , and N=.4, if D < 0.01, else N=.6

The Cise flow boiling critical heat flux model is formulated through

$$q_{CHF} = \frac{5.457}{(39.37D)^{0.333} (p_c/p - 1)^{0.4}} \left(\frac{1 - p/p_c}{(G/1000)} - x\right) \quad (4.15)$$

with $p_c = 221. * 10^5$ Pa for the critical pressure

Table 3. Critical heat by the GENFLO model and values for other selected correlations.

Correlation	q as W/m^2 ,		
	1 bar, 1 m/s	10 bar, 1 m/s	70 bar, 1 m/s
by flow quality,	0.05	0.05	0.05
corresponding void fraction	0.89	0.46	0.092
GENFLO critical heat flux	$0.7x10^6$	$1.2 x10^6$	$2.4 x10^6$
Biasi flow boiling	$5.9 x10^6$	$6.2 x10^6$	$5.7 x10^6$
Cise flow boiling	$3.7 x10^6$	$4.8 x10^6$	$5.8 x10^6$
Griffith-Zuber pool boiling	$4.9 x10^4$	$5.9 x10^5$	$1.5 x10^6$

4.3 Quenching front movement and heat transfer

The heat transfer coefficient decreases across the quenching front by more than 2 orders of magnitude from that of nucleate boiling to that of film boiling. The wall temperature in the quenching front drops several hundreds of degrees from the post-dryout temperatures down to wetted temperatures. The heat transfer takes place as transition boiling heat transfer, but the axial heat conduction in the cladding takes also part in the cooling process. In many systems this short regime with intensive evaporation has been modelled applying the normal transition boiling model, but improved models have included a moving mesh applying the nodes shorter that 1 cm.

In 1970'ies many models for the rewetting were developed in a form of an analytical correlation, where the two-dimensional heat conduction equation was solved for the cladding. By using two fitting parameters, the effective heat transfer on the wetted side and Leidenfrost temperature, the analytical model could be tuned against measured rewetting velocities.

The model developed by Andersen at Risø is expressed through the Biot's number, dimensionless temperature and Peclet's numbers as an expression for the quenching velocity through Biot's number

$$Bi = h_f S_w / \lambda_w \tag{4.16}$$

where h_f is the effective heat transfer coefficient, S_w is the surface perimeter, λ_w is the conductivity of cladding. The dimensionless temperature θ is defined as

$$\theta = \left[\frac{\left(T_w - T_s\right)\cdot\left(T_w - T_0\right)}{\left(T_0 - T_s\right)^2} \right]^{1/2} \tag{4.17}$$

where $T_0 = T_s + \Delta T_L$ is the Leidenfrost temperature, T_s is saturation temperature and ΔT_L is constant temperature difference, Leidenfrost temperature difference, around 160 K, and T_w is the cladding temperature on the dry wall.

The dimensionless temperature has been depicted in Figure 12 as a function of the wall temperature and by varying the Leidenfrost temperature difference ΔT_L.

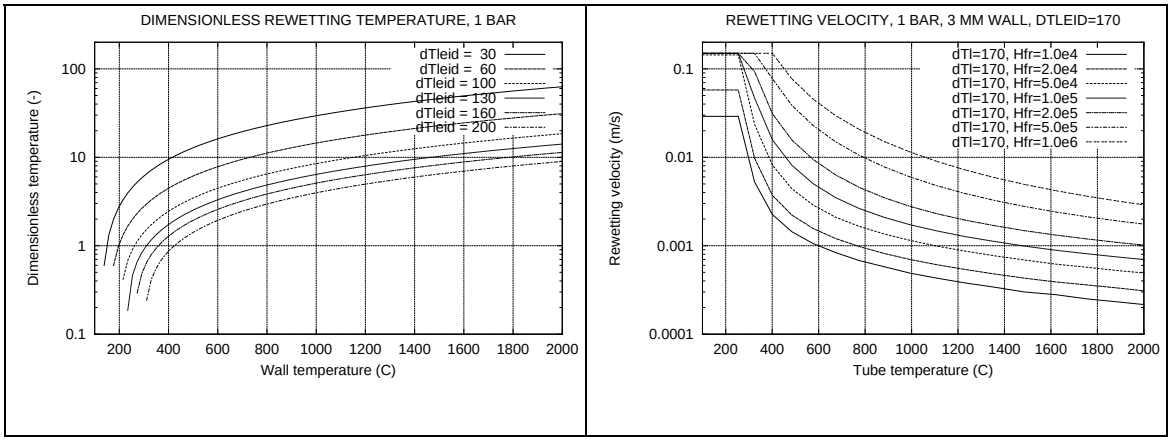

Figure 12. Dimensionless temperature and front velocity.

Andersen developed a fitting for a cylindrical rod geometry giving good values both for the fast and slow rewetting (Andersen & Hansen, 1974). The correlation in a dimensionless form is expressed through

$$Pe = \left\{ \left(\sqrt{Bi}/\theta \right)^3 + 2^{-3/4\sqrt{\pi}} \left(Bi/\theta^{1+\sqrt{\pi}/2} \right)^3 \right\}^{1/3} \tag{4.18}$$

The Peclet's number is further correlated to rewetting velocity through its definition as

$$V_{fr} = \frac{Pe\ \lambda_w}{\rho_w \cdot c_w \cdot S_w} \tag{4.19}$$

where ρ_w is the cladding density, c_w is the specific heat of cladding.

The heat generation of the quenching front is derived assuming the excess capacitive heat, from T_w to T_s in the cladding released into coolant. The expression is not included here, because it is rather complex with heat capacities for two different materials.

In comparison to another expression based on considering a slab geometry instead of a rod geometry was developed also in 1970's by Dua and Tien giving

$$Pe = \left\{ \frac{Bi}{\theta(\theta-1)} \left(1+0.40\times \frac{Bi}{\theta(\theta-1)} \right) \right\}^{0.5} \tag{4.20}$$

The correlation should take into account the reduction in the heat transfer by high void fraction. The quenching front should retreat in the situation, where the wall becomes dry. The situation was solved by defining the limiting void fraction, where the front movement is stopped and above which the front begins to move downwards. The limiting void fraction has been selected as α = 0.985. For making the velocity transitions smooth the wet side heat transfer is reduced as a function of void fraction with the equation

$$h_{fr} = h\ (0.985^5 - \alpha^5)\, s_w / k_w \tag{4.21}$$

The expression gives zero front velocity with void fraction α = 0.985. Above it the velocity is negative, 40 % from the maximum velocity at α = 1.000 and zero velocity at α = 0.985. A linear ramp function is assumed between α = 0.985 and 1.000.

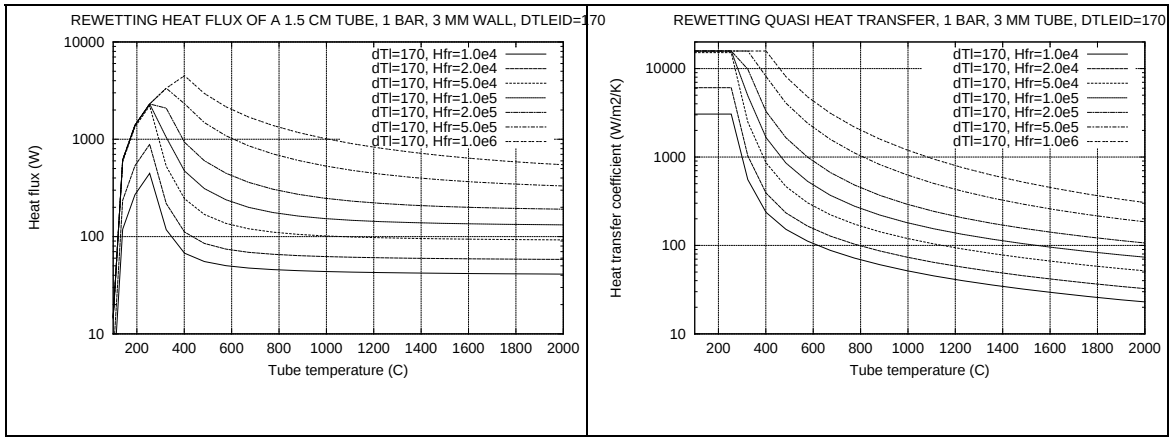

Figure 13. Front heat flux and its interpretation as a heat transfer coefficient for transition boiling.

The quench front velocity is also depicted in Figure 13 as a function of wall temperature for the Leidenfrost temperature difference ΔT_L = 170 K and by varying the wet side heat transfer coefficient *(Hfr=h_f).* By assuming a tube thickness of 3 mm the total heat flux from the quenching front to the coolant is depicted in Figure 13 for a 1.5 cm diameter tube. The result indicates well the increment of the heat transfer coefficient in the vicinity of the quenching front. The rewetting front heat transfer can be interpreted also as an effective heat transfer coefficient and this is done in Figure 13 by assuming the rewetting area is modelled by a 0.1 m long node. It is assumed that the wall is cooled by

a transition boiling correlation from dry temperature to saturation temperature. The results shows clearly, that if the heat transfer in the vicinity of a rewetting front is decribed by a transition boiling heat transfer, the heat transfer rate should increase very strongly by decreasing wall heat transfer.

4.4 Post-dryout heat transfer

As mentioned earlier, six different heat transfer mechanisms are distinguished in the post-dryout regime. The film boiling heat transfer mode was selected for representing the liquid located in the vicinity of the wall, but not contacting it as is assumed for the transition boiling heat transfer. In Table 4 the heat transfer coefficients for two known correlations are listed as functions of pressure. The discrepancy between correlations is rather large.

The reference model by Bromley is formulated through

$$h_{fb} = 0.62\left(\frac{\lambda_g^3 g\rho_g(\rho_l - \rho_g)h_{fg}}{D_e\mu_g(T_w - T_s)}\right)^{0.25} \tag{4.22}$$

The reference model by Berenson is formulated through

$$h_{fb} = 0.425\left(\frac{\lambda_g^3 g\rho_g(\rho_l - \rho_g)h_{fg}}{\mu_g\left(\frac{\sigma}{g(\rho_l - \rho_g)}\right)^{0.5}}\right)^{0.25} \tag{4.23}$$

Table 4. Typical heat transfer values by classical film boiling heat transfer correlations.

Correlation	Use	h as $W/m^2/K^{0.75}$		
		1 bar	10 bar	70 bar
Bromley FB	$q = h_{fb}*(T_w-T_s)^{0.75}$	219.	418.	954.
Berenson FB	$q = h_{fb}*(T_w-T_s)^{0.75}$	672.	1322.	3271.

No existing correlation was selected for the film boiling heat transfer mode. Instead a simple correlation was selected

$$q_{fb} = Ch_{fb}(1-\alpha)(T_w - T_s) \tag{4.24}$$

where: $h_{fb} = 200$ W/m^2/K, the heat transfer coefficient is estimated from the Bromley by taking into account, that the wall superheat is included as a liner parameter instead of

exponentation. The void fraction is assumed to be well representative for the wall having liquid in the vicinity. The recommendations for the coefficient C range from 0.10 to 0.20 based on the validation work.

In discussions about quenching front propagation the transition boiling was seen as one component in the rewetting process, although also an additional term related to the axial heat conduction exists. Transition boiling is in fact one mode of the nucleate boiling, when the wall is wetted only periodically. The contact time becomes longer, when the temperature drops. Because the phenomenon is very local, its accurate calculation is not possible with typical nodalizations. The assumption in any case is, that also this heat transfer mode exists and if the wall temperature drops down to the Leidenfrost temperature, the heat flux is equal to the critical heat flux. If the temperature is higher, the heat flux rate drops quickly. In addition to this the efficiency is proportional to the local void fraction. The expression defined for the transition boiling is

$$q_{tb} = Aq_{chf}\frac{\Delta T_L(T_w - T_s)}{< T_w - T_s, \Delta T_L >^2} = Aq_{chf}\,F_{tb} \tag{4.25}$$

where q_{chf} is critical heat flux calculated by the Equation (4.12). The coefficient A is used for the relative efficiency of the transition boiling process and its recommended range is between 0.10 to 0.30 according to validations. It may be considered, that this correlation takes care of the transition boiling much before the rewetting. The rewetting correlation takes care of the last period before the final contact with the wall.

The transition boiling model is typically included in the system codes and e.g. in RELAP5 the model proposed by Chen has been applied, although with some modifications. The post-dryout heat transfer model in RELAP5 consists of two contributions, transition boiling and steam heating as follows

$$q_{TB} = F_q\,q_{chf} + (1 - F_q)q_{wg} \tag{4.26}$$

In fact the F_q in Equation (4.26) corresponds to F_{tb} in Equation (4.25). The F_q coefficient is defined as follows, following the original model formulation by Chen

$$F_\alpha = \frac{0.005}{1.001 - \alpha^{40}} + .0075\,\alpha \tag{4.27}$$

$$F_G = \max(2.4 - \frac{G}{135.6}, \frac{0.2G}{135.6}) \tag{4.28}$$

$$F_q = \exp(-sqrt(1.8) * F_\alpha * F_G * sqrt(T_c - T_s)) \tag{4.29}$$

In RELAP5 the expression has been modified into the form

$$F_q = \exp(-sqrt(1.8) * F_\alpha * F_G * \min(sqrt(T_c - T_s), 15.0) \tag{4.30}$$

but this deviates from the original formulation. The comparison is made based on the Equation (4.29).

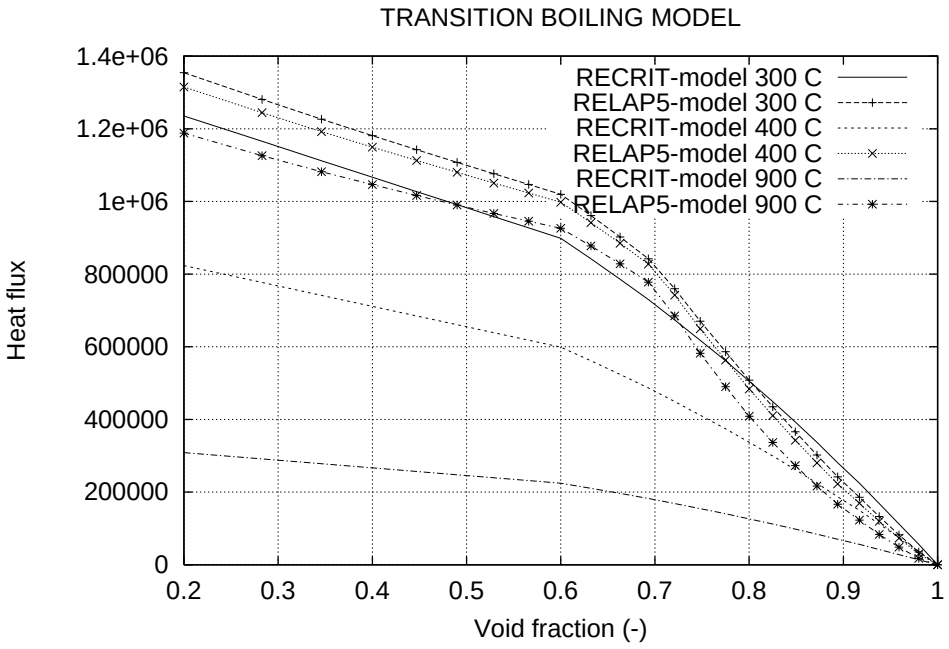

Figure 14. Comparison of transition boiling models calculated with the model used in RELAP5 and GENFLO (RECRIT).

The heat flux of GENFLO and RELAP5 have been compared as a function of the void fraction in Figure 14. The flow velocity was assumed 1.0 m/s and the mass flux was calculated by assuming homogeneous flow conditions. Only the transition boiling contribution was considered for RELAP5 model. The critical heat flux correlations have the same assumptions. The atmospheric pressure is assumed. The comparison proves that by 300 ^{o}C the transition boiling model of GENFLO is rather close that of RELAP5. But at higher wall temperatures the models diverge rather much. The results with the RELAP5 model are affected surprisingly little by temperature. On the other hand GENFLO model includes also a film boiling contribution, which is not included in RELAP5. In principle the heat transfer into gas is similar in both codes. The GENFLO results do not give any confirmation for the transition boiling model in GENFLO for the whole range, but at least for lower temperatures.

In the droplet-dispersed flow regime the first step is the forced convection from the wall to gas. This is calculated analogously with the convection into the stem through

$$h_{cg} = 4.36\, D_h / \mu_g \tag{4.31}$$

if Re < 2000 else Dittus-Boelter correlation is used

$$Re = \frac{W_g\, D_e}{A \mu_g} \tag{4.32}$$

$$h_{gc} = \frac{\lambda_g}{D_e} 0.023 \cdot Re_g^{0.8} \cdot Pr_g^{0.4} \tag{4.33}$$

For simplicity $Pr_g = 1.0$ is assumed.

$$q_{cg} = h_{cg} \cdot (T_w - T_g) \tag{4.34}$$

Radiation heat transfer is calculated assuming only absorption into liquid:

$$h_R = \sigma \cdot \varepsilon \cdot \frac{T_w^4 - T_s^4}{T_w - T_s} = \sigma \cdot \varepsilon \cdot (T_w{}^3 + T_w{}^2 T_s + T_w\, T_s{}^2 + T_s{}^3) \tag{4.35}$$

The more precise formulation for the emissivity is written as

$$\varepsilon = \frac{1}{\frac{1}{\varepsilon_w} + \frac{1}{\varepsilon_l} - 1} \tag{4.36}$$

and this is valid for the situation, where a hot surface is radiating to the liquid. The radiation heat absorption model has been simplified, however. The formula is written as

$$q_{rad} = B\sigma\varepsilon(1-\alpha)(T_w{}^4 - T_s{}^4) \tag{4.37}$$

where emissivity of the wall ε = 1.0 has been assumed. B is user tuning parameter and values B 0.10 to 0.25 are recommended based on the validation work. In the heat transfer between structures the absorption due to liquid is neglected, because its evaluation would require an estimate for the mean beam length.

The radiation heat exchange is solved between two-dimensional core heat structure elements by assuming the effective radiation heat transfer area to be equal to the horizontal flow area between radial rings in vertical direction and the vertical walls between the radial rings in the horizontal direction. The radiation heat flux per unit radiation heat transfer area is expressed by

$$q_R = \sigma \cdot \varepsilon \cdot (T_{w1}^4 - T_{w2}^4)(\Delta r_{rad} / \Delta r_i) \qquad (4.38)$$

The last fraction in the parenthesis describes the resistance of the radiation heat exchange. It is measured as a number of resisting walls located between radiating surfaces. The illustration of radiation conditions in the BWR core is shown in Figure 15.

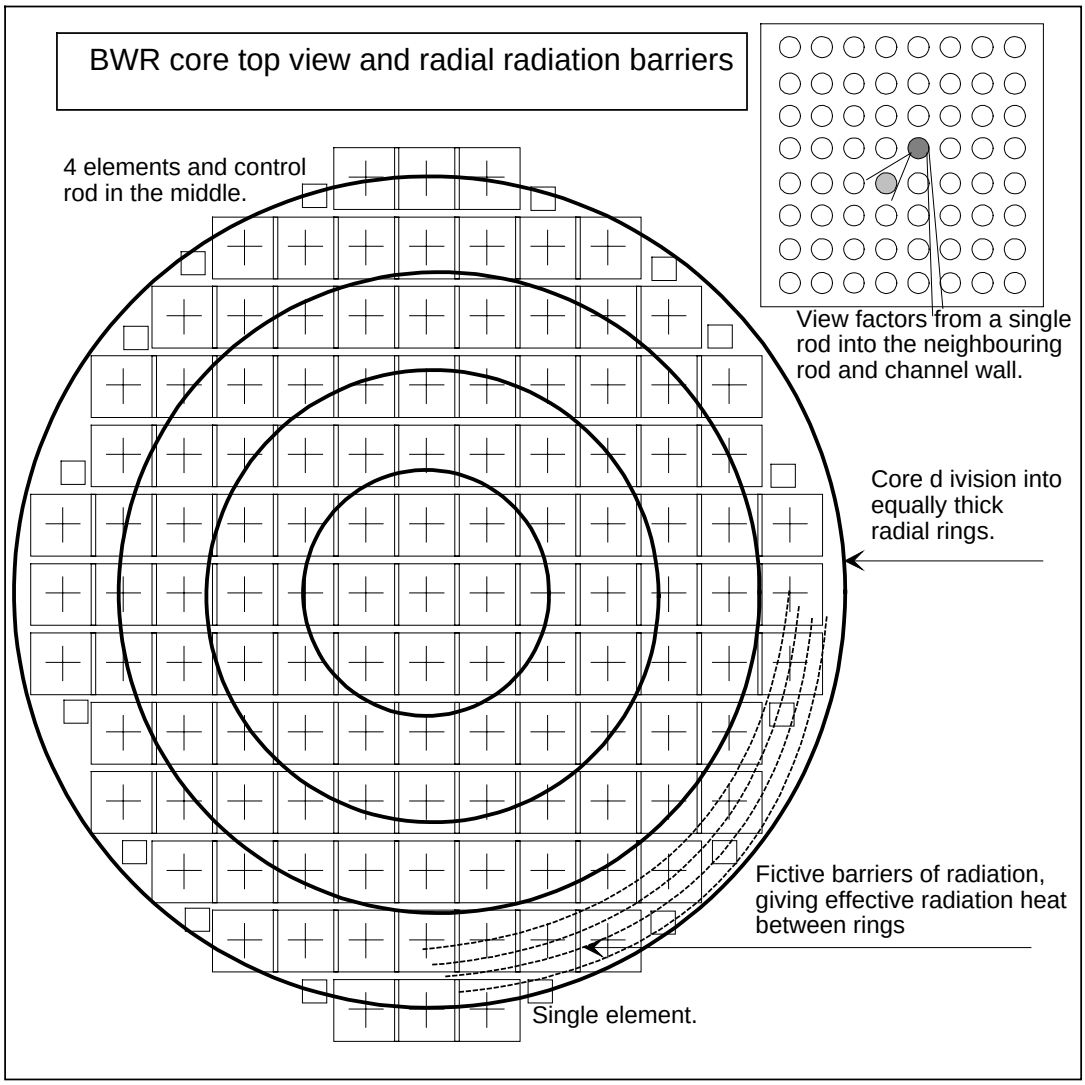

Figure 15. Radiation model applied to the radial description of the BWR core.

Between radiating surfaces with area A = 1 four separating walls are located. The number of separating walls is calculated as $N_w = dR/dr$. The walls between have zero heat capacity. In this situation the heat flux between two surfaces can be defined as:

$$Q_{rad} = h_R(T_1 - t_1) = h_R(t_1 - t_2) = h_R(t_2 - t_3) = h_R(t_3 - t_4) = h_R(t_4 - T_2) = \frac{1}{N_w} h_R(T_1 - T_2) \tag{4.39}$$

The heat transfer coefficient for the radiation is defined by the Equation (4.39). In reality the coefficient changes between each wall, but by assuming the temperature difference between T1 and T2 relatively small the same heat transfer coefficient may be used for each step.

4.5 Interphasial heat transfer

The interphasial heat transfer as flashing, condensation and droplet evaporation are formulated with convection analogy with temperature differences for liquid superheat, liquid subcooling and steam superheating, respectively.

Forced convection from the fuel cladding to the steam and interfacial heat transfer between superheated steam and water droplets are calculated in single phase steam and dispersed liquid regions. Forced convection heat transfer coefficient in the steam region is based on the Dittus-Boelter equation for pure steam.

The interfacial heat transfer between overheated steam and water droplets is calculated by:

$$q_{if} = DC_{if}\alpha(1-\alpha)\rho_l(T_g - T_s) \tag{4.40}$$

where C_{IF} is 1500 W/kg/K. The coefficient C_{IF} has been found to be a good estimate for the heat transfer between gas and 1 mm size droplets with a typical relative velocity in the range of 3 m/s. The coefficient D is a user tuning parameter which has the recommended range from 0.20 to 0.75.

In principle the heat transfer between a single droplet and steam fulfils the heat transfer rate

$$h_{if} = \frac{\lambda_g}{d}\left(3.2 + 0.75\left(\frac{d\,\rho_g \Delta u}{\mu_g}\right)^{0.8} \mathrm{Pr}_g^{\,0.33}\right) \tag{4.41}$$

At 5 bar, ($\mu_g = 1.3*10^{-5}$ kg/m/s, $\lambda_g = 0.030$ W/m/K) with velocity difference of 5 m/s, and droplet diameter 0.003 the heat transfer coefficient becomes $h_{if} = 4428$ W/m^2/K.

The droplet surface area per unit volume may be expressed through

$$A_d = \frac{1-\alpha}{d} V \tag{4.42}$$

This gives the heat transfer coefficient for 3 mm droplets and 5 m/s velocity difference the values of $1.47*10^6$ *(1-α) W/m^2/K. The value corresponds quite well to the basic interfacial heat transfer.

The droplet size relationship with respect to the relative velocity may be derived from the combination of the interfacial shear and Weber number criteria

$$C_d = \max(0.4 + 25.4/(\frac{d\,\rho_g \Delta u}{\mu_g})^{0.8},\ 24.0/(\frac{d\,\rho_g \Delta u}{\mu_g})) \tag{4.43}$$

$$\Delta u = sqrt(\frac{4\rho_l\, d\, g}{3\rho_g\, C_d}) \tag{4.44}$$

$$We = \frac{4\rho_g\, \Delta u^2 d}{\sigma} \tag{4.45}$$

The recommended Weber number for droplet flow is 6.5, based on the spray experiments. By this values of the droplet size at 3 bar would be 3.5 mm and the relative velocity 7.8 m/s between the gas and droplets.

The interphase heat transfer is calculated for flashing and condensation by using a constant interphase heat transfer coefficient. The similar procedure is done for all sections and in the primary section separately for the cold and hot zones. The basic assumption is that the flashing delay related to the nucleation delay is not considered. It is important during the first second of the large break LOCA. For flashing of the superheated liquid

$$q_{fl} = 1500(1-\alpha)\rho_l\, max(T_l - T_s, 0) \tag{4.46}$$

$$\gamma_i = q_{fl}/(h_{gs} - h_l) \tag{4.47}$$

The coefficient 1500 has been found well functioning for the calculation of small break LOCA or medium break LOCA depressurisation. But for the large break LOCA a higher value may be needed for preventing too large liquid superheats in the rapid depressurization.

For condensation of the vapour into the subcooled liquid the model is simply defined through

$$q_{co} = 1000.(1-\alpha)\rho_g \rho_l \alpha \ \max(T_s - T_l, 0) \tag{4.48}$$

$$\gamma_i = -q_{co} / (h_{gs} - h_l) \tag{4.49}$$

The simple correlation possible to be dialled by the used was found better than the empirical correlations applied in the system code.

The correlations by Shah is one used in system codes and it is written through

$$h_{cn} = 4.0 \times C_1 (4.0 + 0.023 Re^{0.8} \ Pr^{0.4}) C_2 \frac{\lambda_l}{D_e^{\ 2}} \tag{4.50}$$

$$C_2 = 1. + 3.8 \left(\frac{\alpha \rho_g (p / p_{cr})^{0.38}}{((1-\alpha)\rho_l)^{0.76}} \right.$$

$$C_1 = \frac{30(\alpha - \delta) + 1800 (\alpha - \delta)^2}{((1 + 30(\alpha - \delta))(1 + 60\alpha^2 - 0.081(p / p_{cr})^{0.38} \alpha^{1.76} (1-\alpha)^{0.3}))}; \ \delta = 10^{-5}$$

The correlation takes into account the flow conditions in the channel and effect of the flow velocity to the condensation rate is dominant. But in the vicinity of the pool boiling conditions the functioning of this model is rather uncertain. Thus no flow dependent model was favoured in GENFLO.

In RELAP5 the condensation model for the bubbly flow regime is defined by the Unal modle through

$$h_{cn} = 1.8 \alpha C \Phi h_{fg} \frac{\rho_l \rho_g}{\rho_l - \rho_g} \ ; \Phi = 1.0 \ \text{if } v_l < 0.6; \ \Phi = 1.639344 \ v_l^{0.47}, \text{ if } v_l > 0.6 \tag{4.51}$$

$C = 65 - 5.69 \times 10^{-5} (p - 1.0 \times 10^5)$; if p<1 MPa and

$C = 2.50 \times 10^9 / p^{1.418}$ if p > 1 Mpa.

In this model the velocity term is weaker than in the Shah model, but still important. Neither this model was seen applicable for the present version of GENFLO. But if needed, the simple condensation model could be replaced by one of the models discussed here or alternative models.

4.6 Phase separation

The phase separation is solved through the basic Equation (3.6). The parameter drift flux velocity v_{gj} describes the phase separation caused by gravitational forces. The phase separation for the bubble flow based on the Zuber-Findlay drift flux correlation could be described by the Equation (4.52).

$$v_{gj}=1.53\left[\frac{g\sigma\Delta\rho}{\rho_l^2}\right]^{1/4} \tag{4.52}$$

The distribution parameters is defined as

$$C_o=\frac{\langle\alpha\, j\rangle}{\langle\alpha\rangle\langle j\rangle}=1.2 \tag{4.53}$$

The expression in the brackets (<>) means a cross section averaging, i.e. <> = ∫dA/A. Note that the basic formula for the drift flux model is written for the velocity, not for the mass flux. In principle the velocity itself is not strongly pressure dependent.

The parameter C is the distribution parameter describing the homogeneous character of the flow. For homogeneous void fraction over the cross section C = 1. For distributed void fractions, e.g. for annular flow C > 1, typically C=1.0...1.3. For subcooled boiling with droplets standing on the wall C < 1.

Table 5. Flow regimes related to distribution parameter of the drift flux model.

Co	
1	Homogeneous flow
> 1	Slip flow
< 1	Bubbles attached on the wall
> 1	Void at the center

The original drift-flux model is based on the bubble flow regime and it gives rather flow relative velocities between steam and liquid in the typical reactor channels.

But the basic expression being valid for the bubble flow regime is not satisfactory for the reflooding flow patterns ranging from the droplet flow to the droplet-dispersed mixture flow. Quite much proposals may be found from the literature for drift flux velocities in reactor condition, especially for the core. One correlation proposed by

Maier and Coddington (Maier & Coddington, 1997) as the best fit correlation for the reactor core conditions may be expressed as follows

$$V_{gj}=(6.73\times10^{-7}\cdot P^2-8.81\times10^{-5}\cdot P+1.05\times10^{-3})\cdot G+ (5.33\times10^{-3}\cdot P^2-1.823\times10^{-1}\cdot P+8.00\times10^{-1}) \quad (4.54)$$

$$C_o=2.57x10^{-3}\cdot P+1.0062 \quad (4.55)$$

P is pressure as MPa, G is mass flux density as kg/m^2/s. Both models have some weaknesses. The relative velocities become quite large by large void fractions. The Maier / Coddington model is strongly dependent on the mass flow rate. This feature increases the risk for an oscillatory solution.

The EPRI correlation is generally considered as the most wide range correlation for the different flow regimes in the simple tube and fuel bundle geometries. The correlation is written through

$$V_{gj}=1.41\left[\frac{g\sigma\Delta\rho}{\rho_l^2}\right]^{1/4}(1-\alpha)^{K_1}C_2C_3C_4 \quad (4.56)$$

with

$$K_1=B_1 \text{ if } \mathrm{Re_g} > 0.0, \text{ else } K_1=min(0.65,0.5exp(\frac{Re_g}{4000}))$$

$$C_o=\frac{L(\alpha,p)}{K_o+(1-K_o)\alpha^r},\ C_1=\frac{4\,p_{crit}^{\ 2}}{p(p_{crit}-p)},\ C_2=1.0,$$

$$C_3=max(0.50,2\times exp(-\frac{Re_l}{60000})),\ C_4=1.0,\ Re=max(\frac{u_g\rho_g D}{\mu_g},\frac{u_l\rho_l D}{\mu_l}),$$

$$B_1=1/(1+exp(\frac{-Re}{60000})),\ B_1=min(0.8,B_1),\ K_0=B_1+(1-B_1)(\rho_g/\rho_f)^{1/4},$$

$$r=(1+1.57(\rho_g/\rho_f))/(1-B_1).$$

The model is rather comprehensive for modelling the co-current and counter-current phase separation in diverse geometries for the stationary flow. In the flow channel the

void fraction and velocity changes may be so drastic that this kind of complex model may be easily the source of the numerical oscillations.

After a through study of different drift flux models a simple approach was selected for the GENFLO code. It was found that for the core channel the drift flux velocity V_{gj0} = 0.8 m/s and the distribution parameter C_{00} = 1.05 are rather well representative for the reactor flow channels at medium and high void fractions. But numerically the drift flux model gives very high relative velocities, when the void fraction approaches the value 1.0. At high void fraction, typically above 0.9 the droplet dispersed flow is most dominant in accident situation, when the dryout has been occurred. In this case the droplet size in the range of 1−3 mm, and with these droplets the relative velocity may be calculated based on simple droplet gas correlations. Based on these conclusion the drift flux model into GENFLO was formulated by applying rather simple principles:

1. The drift flux velocity and the distribution coefficient are constant, typically V_{gj0} = 0.8 m/s and C_{00} = 1.05, for the low and medium void fraction ranges.

2. The relative velocity calculated with the drift flux model and the above coefficients reaches at the relative velocity for the 3 mm droplets at the void fraction 0.85.

3. Above the void fraction 0.85 the drift flux model is formulated in such a way that the relative velocity is constant for the void fraction 0.85 to 1.0.

The formulation fulfilling these conditions was formulated through following equations

$$V_{gj}=V_{gj0}\ min(\frac{1-\alpha}{0.15},1.0) \tag{4.57}$$

$$C_o=1+(C_{oo}-1)\,min(\frac{1-\alpha}{0.15},1.0) \tag{4.58}$$

where V_{gj0} = 0.3 … 1.2 and C_{00} = 1.02 … 1.15. By using V_{gj0} = 0.8 and C_{00} = 1.05 the results depicted in Figure 16 for the relative velocity can be achieved.

A special emphasis in the simplified model is, that the relative velocity is limited on the high void fraction area. This means droplet dispersed flow, where, the interfacial shear between droplet and vapour define the relative velocity. This is an advanced feature compared to other proposed models. A convenient feature is, that the mode used is controlled through two constants.

The droplet size relationship with respect to the relative velocity has been evaluated in Equations (4.43), (4.44) and (4.45). The relative velocity in the range of 8 m/s may be

expected for the droplet dispersed flow. The GENFLO model gives reasonable results against this criteria.

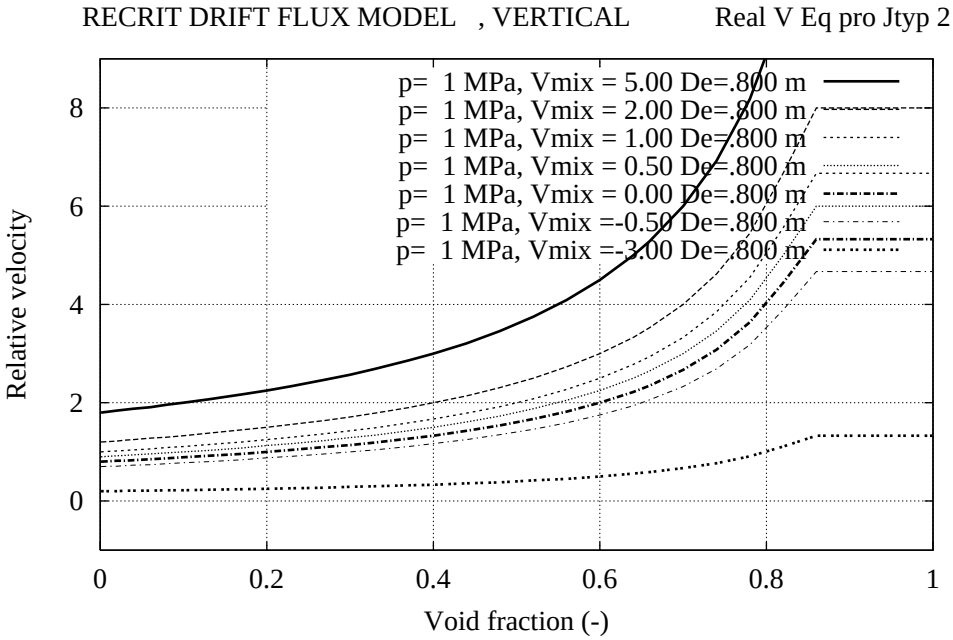

Figure 16. The relative velocities as a function of the volumetric flow rate as a function of the void fraction, by assuming C = 1.05 and Vgj = 0.8.

The selection criteria for the drift flux model may be summarised as follows:

- No correlation with mass flow rate has been used. The drift flux model is an expression for the relative velocity, not for the mass flow.
- The model should be valid also for the down flow.
- Droplet dispersed flow is assumed for the high void fraction, droplet carried by steam and relative velocity from equation above.
- The low flow area fitting to the bubble and slug flow models.
- No droplet detachment in the boiling channel considered.

4.7 Wall friction

The basic wall friction is defined from the empirical correlation which in the most simple form for the single phase flow can be defined as

$$f_{wl} = \frac{0.375 \mathrm{Re}_l^{0.8}}{D_e} \tag{4.59}$$

This model may be used for the estimation of the friction for the smooth wall. Additionally singular loss coefficients have to be used in the contractions.

The two-phase multiplier is typically an empirical correlation fitted to the experimental data. By assuming a homogeneous flow the multiplier is expressed as

$$F_{TP} = \frac{\rho_l}{\rho_m} \tag{4.60}$$

A singular loss coefficient may be given in flow connections between different sections. For the smooth wall the wall friction is given as constant with fully developed turbulent flow f = 0.02 may be recommended. In addition it has been assumed, that F_{TP} = 1.0. Especially in the post-dryout regime the velocities are high and there the wall is in contact only with vapour, not with liquid. The friction is defined by the steam velocity. In this situation it is difficult to believe, that the two-phase multiplier based on the liquid density could be valid.

5. Heat structure integration

5.1 Solution of averaged temperatures

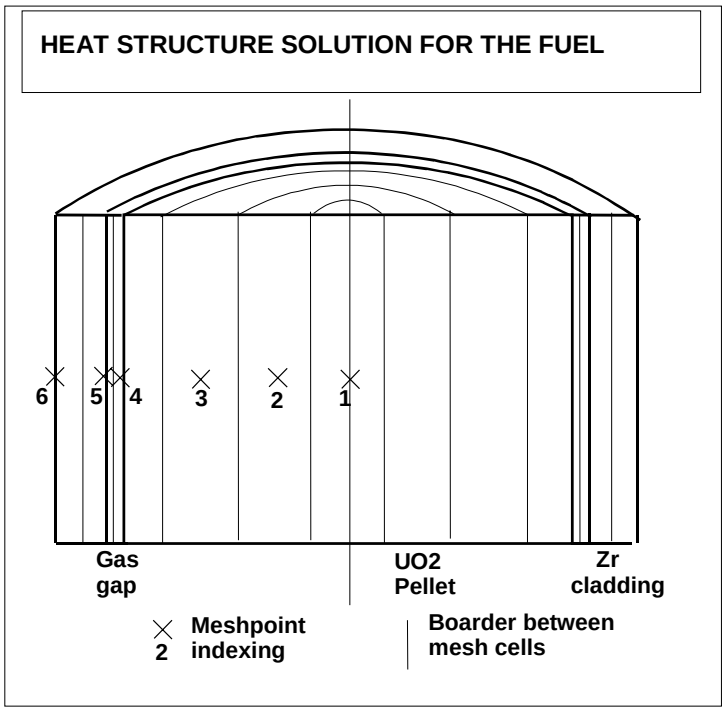

Figure 17. Radial mesh point distribution for the fuel rod.

The solution based on the average fuel pellet and cladding temperatures is an optional solution in GENFLO. In this case the transient heat conduction equation for the radial conduction is solved in an integrated form for the fuel pellet and cladding. The method allows, however, the computation of the radial temperature distribution described with key values, like fuel centre temperature, gas gap temperature and cladding surface temperature. The average temperatures are defined for the cladding and fuel pellet. The cladding is coupled to the fluid by the heat transfer correlation. The fuel pellet is coupled to the cladding through the heat transfer coefficient over the gas gap. The radial mesh division is depicted in Figure 17.

The approach for the average temperatures is based on consideration of steady state conditions. The heat conductions are inverted into resistances. By assuming that the power generation inside the pellet is constant per unit volume a relationship between the power generation inside a ring and temperature gradient at the distance r may be defined through

$$2\pi r\lambda\frac{\partial T}{\partial r}\Delta z=-q'''\pi r^2\Delta z \tag{5.1}$$

Integrating this from the center-line to the distance r a temperature profile can be defined through

$$T(r)=T_{\max}-q'''\frac{r^2}{4\lambda_f} \tag{5.2}$$

The Equation (5.2) can be integrated over the pellet giving the average fuel pellet temperature and its expression is written as

$$T_{av}=0.5(T_{\max}+T_{\min}) \tag{5.3}$$

The heat transfer coefficients can be coupled together via resistances in the following way

$$\frac{1}{h_{tot}}=\frac{1}{h_f}+\frac{1}{h_g}+\frac{1}{h_c} \tag{5.4}$$

$h_{fuel}=$ heat transfer coefficient from pellet surface to average fuel, W/m^2/C
$h_{gap}=$ heat transfer coefficient in the gap, W/m^2/C
$h_{clad}=$ heat transfer coefficient in the cladding, W/m^2/C

The average fuel resistance may be defined as

$$R_f=1/h_f=r_p/(4\lambda_f) \tag{5.5}$$

The resistance over the gas gap may be defined as

$$R_g=1/h_g=\Delta r_g/\lambda_g \tag{5.6}$$

The resistance over the cladding may be defined as

$$R_c=1/h_c=r_o\ln(r_o/r_i)/\lambda_c \tag{5.7}$$

The lumped volume equations to be solved for the fuel pellet are written as

$$\frac{\rho_f c_f V_f (T_f^{n+1} - T_f^n)}{\Delta t} = Q \; - \frac{(T_f^{n+1} - T_c^{n+1})}{(\frac{R_f}{A_f} + \frac{R_g}{A_g})} \tag{5.8}$$

Note that the heat resistance over the gas gap is summed with the heat resistance over the fuel. The lumped volume equations for the cladding are derived through

$$\frac{\rho_c c_c V_c (T_c^{n+1} - T_c^n)}{\Delta t} = -(Q_w + \frac{\partial Q_w}{\partial T_w}(T_c^{n+1} - T_c^n)) + \frac{(T_f^{n+1} - T_c^{n+1})}{(\frac{R_f}{A_f} + \frac{R_g}{A_g})} \tag{5.9}$$

The equations (5.8) and (5.9) include two unknown temperatures, the fuel temperature and the cladding temperature for the new time step. These temperatures can be solved arithmetically form the equations.

The lumped fuel temperature integration has been realized in the module TFUEA. The average solution mode is selected by the IHSMOD = -1 or +1 in the input data.

5.2 Material data for fuel heat structures

Parameter data table PAR(30) includes several material properties, which may be defined by the user. Additionally the material property package MATPRO may be used for the definition of the specific heat and conductivity of the fuel pellet, zirconium and zirconium oxide. All data is taken from the PAR(30) table, if the integration option IHMOD < 0, i.e. IHSMOD = -1 or –2. In the table following data and their typical values are given:

Table 6. Material properties for the solid fuel structure.

PAR index	Name	Meaning	Unit	Typical value
1	ROCLAD	Cladding density	kg/m^3	6500
2	CPCLAD	Cladding specific heat	J/kg/K	540
4	CONDCL	Cladding conductivity	W/m/K	20.1
5	CONFUE	Fuel conductivity	W/m/K	5.4
7	GAPCO	Gas gap conductivity	W/m/K	0.234
8	ROFUEL	Fuel density	kg/m^3	11000.
9	CPFUEL	Specific heat of fuel	J/kg/K	271.

The MATPRO values are used for the specific heat and heat conductivity, if IHSMOD > 0, i.e. IHSMOD = +1 or +2. In Figure 18 the MATPRO values are depicted for the specific heat and also for the heat conductivity.

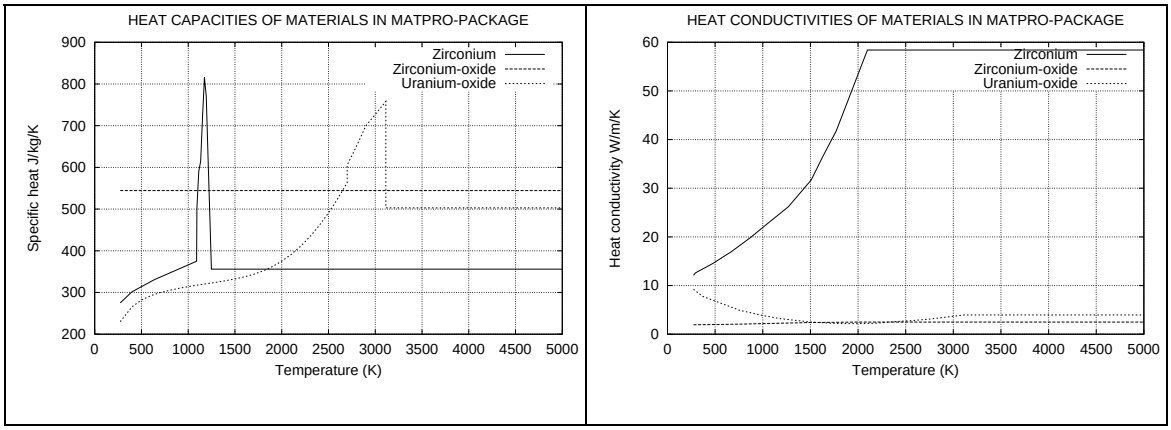

Figure 18. Specific heat and conductivity of fuel, zirconium and zirconium oxide calculated by the MATPRO module.

6. Plant component models

6.1 Mass flow through valve and time dependent friction

The code models the operation of different valves from the steam line into the containment in the following way:

- Relief valve opening as a function of pressure
- Safety valve opening by a pressure hysteresis characteristics
- Time dependent valve position as a function of time

Valve mass flow rate is calculated from a model based on the quadratic pressure loss in the valve as a function of mixture mass flow rate. The friction coefficient is determined from the design flow rate at the nominal pressure. The formula for the valve mass flow rate is given by the Equations (6.1) and (6.2):

$$W_g = \sqrt{\frac{(p - p_{out}) \cdot \rho_g}{X_k}} \tag{6.1}$$

$$X_k = x_k / A_v^2 \tag{6.2}$$

where X_k is pressure loss coefficient defining the mass flow as a function of the pressure loss and the mixture density and including the valve flow area.

6.2 LPIS and HPIS injection

The high pressure injection for a real BWR system can be considered constant. Thus this injection is typically modelled through a time dependent injection.

The LPIS pump head ranges in BWR typically from 0 to 10 bar and in this case pump injection has be modelled as a function of the system pressure. The pump injection may be defined through a simplified pump characteristics, where three pairs of pressure and flow rate are given. An example of three injection points is listed in the Table 7.

Table 7. Three point definition for the parabolic injection curve, low pressure injection.

Point	p (Pa)	W (kg/s)	Type of point
1	1.e5	110.	Lowest pressure, highest flow
2	5.e5	60.	Middle point
3	10.e5	0.	Shutoff pressure, zero flow

The pump characteristics are based on the assumption of a quadratic polynomial between the flow rate and pressure in the section. For low pressure injection this polynomial is derived as

$$p=F_0 + F_1 W_1 + F_2 W_2^2 \tag{6.3}$$

The injection flow rate is calculated as a root of this parabola from

$$W_{LPIS}=\frac{-F_1 - \sqrt{F_1^2 - 4F_2(F_0 - p)}}{2F_2} \tag{6.4}$$

The coefficients F can be defined from three pressure / injection pairs, as

$$F_2 = \min(0.0,(\frac{p_1 - p_2}{W_1 - W_2} - \frac{p_2 - p_3}{W_2 - W_3})/(W_1 - W_3)) \tag{6.5}$$

$$F_1 = (\frac{p_1 - p_2}{W_1 - W_2}) \tag{6.6}$$

$$F_0 = p_1 - F_2 W_2^2 - F_1 W_1 \tag{6.7}$$

7. Code programming

In the principle of integral momentum solution, the steam density and saturation temperature are only functions of the system pressure in the loop. In this way the acoustic effect on the steam density is filtered away and the saturation temperature, affecting the steam generation, does not depend on the local pressure The system pressure is attached to the steam dome. All evaporation rates and pressure components of the density depend only on this pressure. It is solved as an integrated quantity for the whole vessel volume.

Additionally the assumption is made that also the local pressure distribution is solved. It is needed for calculating the circulation momentum equations in predefined locations. These momentum locations are in the core inlet, one momentum equation into each fuel channel, in the bypass inlet and the recirculation connection from the steam separator into the downcomer. The number of momentum equations needed for the circulation is equal to the number of parallel loops, i.e. degree of freedom in the system.

The momentum equation is solved for the volumetric mixture flow. After the volumetric flow is solved in momentum junction, the volumetric flow distributions are fixed also in the other junctions. This is possible, because the system pressure solution is fixing the densities.

The basis equations and constitutive models are solved in the following order without any iteration over the whole solution system:

1. Define leak, injection and heat source boundary conditions.
2. Predict heat and mass transfer.
3. Create mass error term.
4. Solve system pressure.
5. Update densities, saturation temperature, heat transfer and mass transfer by a new system pressure.
6. Solve pressure distribution.
7. Solve the equation of the circulation momentum.
8. Solve volumetric flow distribution.
9. Find phase separation by a drift flux model.
10. Define phase mass flow rates.

11. Integrate mass conservation, explicit integration.
12. Integrate gas and liquid enthalpy conservation.
13. Integrate the concentration of noncondensable gases
14. Update material properties.

The node and junction indexing is arranged in such a way that all junction flow rates can be solved in the ascending order of junction indices and pressure distribution in descending order without specific manipulations. The node index = 1 is located in the bottom of the core, ring 1, the highest index in the steam dome. The lowest junction index is the core inlet junction into the ring 1 and the highest index the last junction before the system pressure node.

By marching over junction indexes in the descending order the local pressure distribution can be solved based on the earlier solved node. By marching the junction indexes in the ascending order the volumetric flow distributions can be solved based on the earlier solved flow rates. The convention related to the calculation level nodes is depicted in Figure 19.

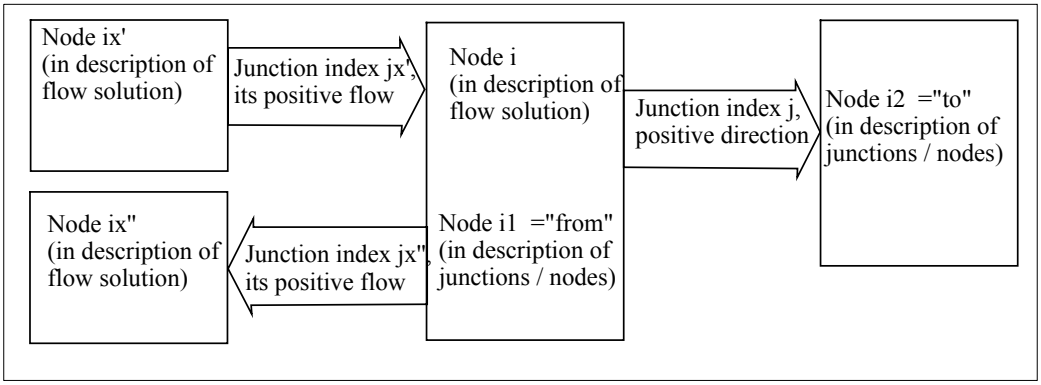

Figure 19. Notation related to the calculation level nodes and junctions.

The convention is known as a staggered mesh applied for one-dimensional geometries. All flow state quantities are related to the nodes, including pressure, phase mass, enthalpy and concentration of noncondensables. All flow quantities are related to junctions, including volumetric flow and phase mass flows.

The pressure distribution and volumetric flow distribution need indexing in a specific order for nodes and junctions in order to avoid matrix solutions. The indexing order is defined automatically in the initialization. Afterwards e.g. the phase flow rates and enthalpies may be solved in a simple loop, meaning the Gauss-Seidel iteration. It is

done for some quantities in the forward and backward direction. For some quantities a single loop is enough. The solutions apply upwind discretization for flow convection and then the time is not limited by the Courant criteria.

8. Validation of GENFLO's reflooding model

The reflooding model of GENFLO has being validated against several experiments (Miettinen, 1999) as a part of the RECRIT development. Related to earlier design base accident studies, a lot of data is available from experiments where the initial temperature before reflooding ranges from 600 to 1000 ^{o}C. The experiments in ERSEC7, FLECHT, GÖTA, ACHILLES, REWET-II and QUENCH facilities were selected for validation of the reflooding capabilities under these conditions. The shematic presentations of the facilities are shown in Figures 20, 21 and 22 and in Table 8 the parameter ranges of the used experiments are summarized.

Table 8. Reflooding experiments used for validating GENFLO (RECRIT application).

Facility	Fuel Length (m)	T_{max} (^{o}C)	Pressure (bar)	Quench time (s)	Rise velocity (m/s)
ERSEC -7, France (2 tests)	1 rod 3.3 m	870	1, 3	1300, 750	0.055
ACHILLES, UK (1 test), PWR	69 rods 3.6 m	1050	3	370	Gravity feed
REWET-II, Finland , PWR (2 tests)	19 rods 2.4 m	910	1, 3	250–500	0.02–0.10
GÖTA, Sweden, BWR (14 tests)	64 rods 3.6 m	950	1, 3,7	600–900	0.008–0.024
FLECHT, USA, BWR(4 tests)	49 rods 3.6 m	790	1, 4, 6.7, 20	50–150	0.076
QUENCH, Germany (2 tests)	21 rods 1.0 m	2100	2	200 < 700 ^{o}C	0.015

The validation results were used for tuning the rewetting and post-dryout heat transfer parameters. The tuning process is discussed in detail in the RECRIT validation report (Miettinen, 1999). The parameter values in Table 9 are recommended for reflooding and recriticality calculations mostly based on the FLECHT-calculation, which investigates a wide pressure range.

Table 9. Overall recommendation for heat transfer, phase separation and oxidation model parameters based on the RECRIT validation work.

Parameter	1 bar	3-4 bar	6-7 bar	20 bar
Rewetting heat transfer coeff [$W/m^2/K$]	1.0–5.0E5	1.7–2.0E5	1.6E5	1.5E5
Leidenfrost temperature difference [K]	160	160	160	160
D in Equation for interphasial heat transfer	0.35–0.75	0.18–0.55	0.50	0.40
C in Equation for film boiling	0.12–0.20	0.10–0.16	0.12	0.10
A in Equation for transition boiling	0.12–0.3	0.15–0.16	0.12	0.10
B in Equation for radiation	0.12–0.25	0.08–0.20	0.14	0.10
Basic drift flux velocity V_{gj0} [m/s]	0.8	0.7–0.8	0.8	0.8
Drift flux separation constant C_0 [-]	1.05	1.05–1.1	1.05	1.05

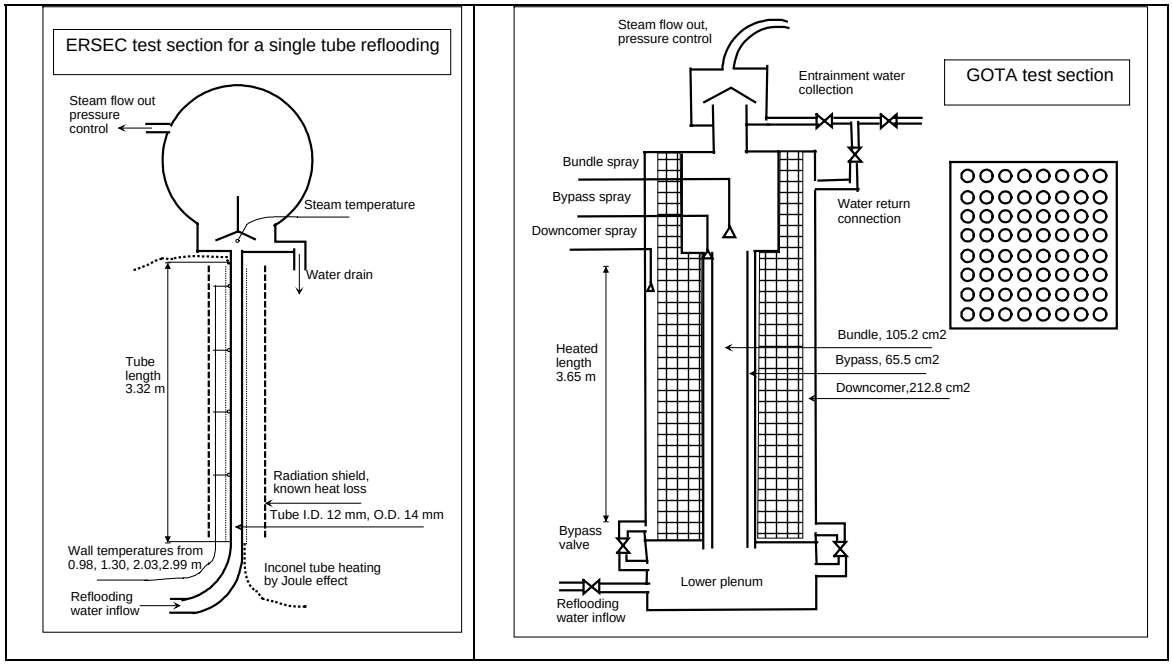

Figure 20. Schematic presentations of the ERSEC and GOTA facilities, used for the validation of the GENFLO thermohydraulics.

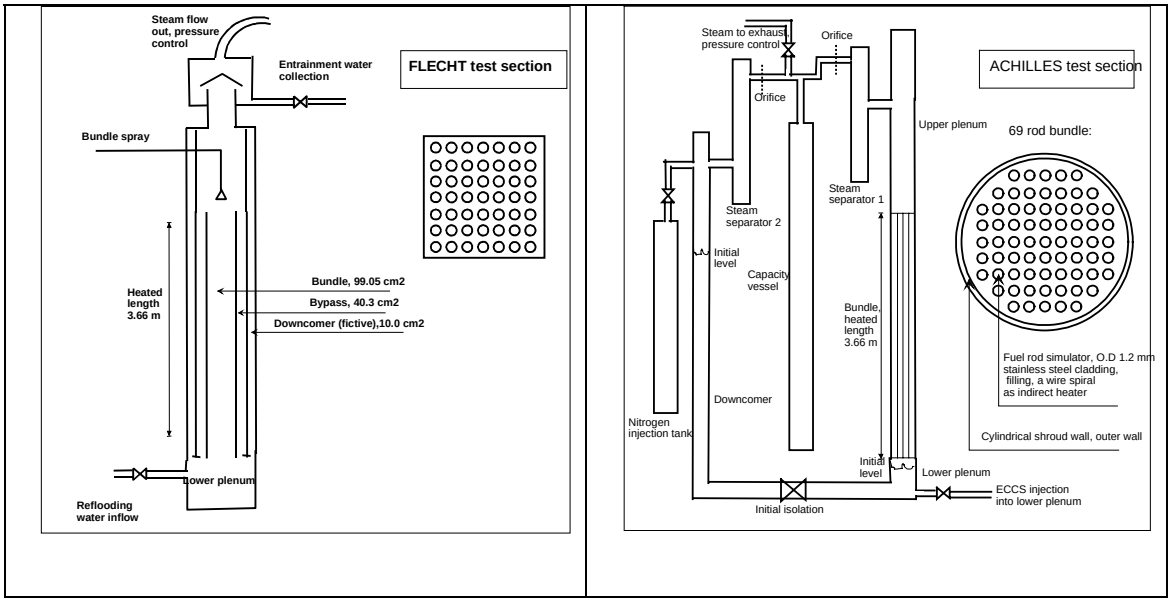

Figure 21. Schematic presentations of the FLECHT and ACHILLES facilities, used for the validation of the GENFLO thermohydraulics.

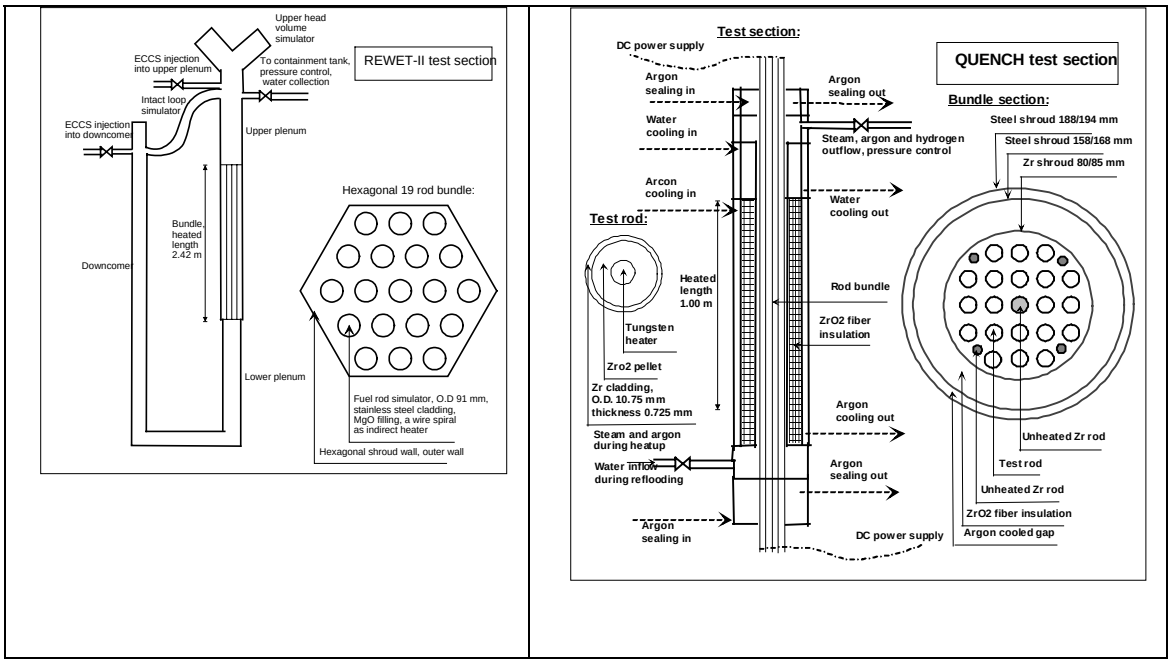

Figure 22. Schematic presentations of the REWET-II and QUENCH facilities, used for the validation of the GENFLO thermohydraulics.

References

Andersen J.G.M. & Hansen P. 1974, Two-Dimensional Heat Conduction in Rewetting Phenomena, NORHAV-D-6, Danish AEC.

Cunningham, M.E., Beyer, C.E., Medvedev, P.G. & Berna, G.A. 2001, FRAPTRAN: A Computer Code for the Transient Analysis of Oxide Fuel Rods, NUREG/CR-6739, Vol. 1, PNNL-13576. Pacific Northwest National Laboratory, Richland, Washington.

Daavittila, A., Kaloinen, E., Kyrki-Rajamäki, R. & Räty, H. 2000, Validation of TRAB-3D Against Real BWR Plant Transients, Proceedings of International Meeting on "Best-Estimate" Methods in Nuclear Installation Safety Analysis (BE-2000), November 2000, Washington, DC.

Hämäläinen, A. Stengård, J-O., Miettinen, J. & Kyrki-Rajamäki, R. 2001a, Coupling of GENFLO thermohydraulic model with FRAPTRAN code for fuel transients. In: Proceedings of the ENS TopFuel 2001 Conference on Nuclear Fuel: Development to meet the challenge of a changing market. Stockholm, Sweden, 28–30 May, 2001 [CD-ROM]. Stockholm: Swedish Nuclear Society. Paper P1-14. 16 p.

Hämäläinen, A., Stengård, J-O., Miettinen, J., Kyrki-Rajamäki, R. & Valtonen, K. 2001b, Coupled Code FRAPTRAN - GENFLO for Analysing Fuel Behaviour during PWR and BWR Transients and Accidents, to be published in proceedings of IAEA Technical Committee Meeting on Fuel Behaviour under Transient and LOCA Conditions, 10–14 September 2001, Halden, Norway.

Kyrki-Rajamäki, R. 1995, Three-dimensional reactor dynamics code for VVER type nuclear reactors, VTT Publications 246, VTT Energy, Finland. ISBN 951-38-4784-5.

Lundström, P., Kymäläinen, O., Myllymäki, S., Raiko, E., Routamo, T., Salminen, K., Silde, A., Toppila, T., Tuomisto, H. & Ylijoki, J. 2001, APROS SA for operator training of Loviisa SAM strategy. OECD Workshop on Operator Training for Severe Accident Management and Instrumentation Capabilities During Severe Accidents, Lyon, France, 12–14 March, 2001.

Maier D. & Coddington P. 1997, Review of Wide Range Void Correlations Against an Extensive Database for Rod Bundle Void Measurements, In: ICONE-5: Fifth International Conference on Nuclear Engineering. Nice, France, May 1997.

Miettinen J. 1999, Validation of thermohydraulics in the RECRIT BWR-recriticality Code, Technical Report MOSES-8/99, September 1999.

Miettinen, J. & Hämäläinen, A. 2000a, Development and Validation of the Fast Running Thermohydraulic Model SMABRE for Simulator Purposes. In: ICONE-8: Eight International Conference on Nuclear Engineering. Baltimore, USA, 2–6 April, 2000 [CD-ROM]. New York: American Society of Mechanical Engineers. Paper ICONE8-8188, 12 p. ISBN 0791819922.

Miettinen, J., Hoejerup, F., Frid W. & Lindholm, I. 2000b, RECRIT Code for BWR Recriticality Analysis, In: ICONE-8: Eight International Conference on Nuclear Engineering. Baltimore, USA, 2–6 April, 2000 [CD-ROM]. New York: American Society of Mechanical Engineers. Paper ICONE8-8189, ISBN 0791819922.

Miettinen, J., Hämäläinen, A. & Pekkarinen, E. 2002, Generalized Thermohydraulics Module GENFLO for Combining with the PWR Core Melting Model, BWR Recriticality Neutronics Model and Fuel Performance Model. In: ICONE 10: Tenth International Conference on Nuclear Engineering. Washington, D.C., USA, 14–18 April, 2002 [CD-ROM]. New York: American Society of Mechanical Engineers, 2002. Paper ICONE10-22421, 14 p. ISBN 0791835898.

Puska, E. K. 1999, Nuclear reactor core modelling in multifunctional simulators, VTT Publications 376, VTT Energy, Finland. ISBN 951-38-5361-6.

APPENDIX – I: Structure of the GENFLO code

Main Main level calls Subroutines Task modules Functions

```
GENFLO
      |< ---      RECRE / RECFR / RECSA
      |< ---      INITRE / INITFR / INITSA
      |< ---      SPOOLI
      |< ---      THYDIN
      :                  |< ---------- INPNOD / INPFRA / INPAPR
      :                  |< ---------- INPSPE
      :                  |< ---------- INPSPA
      :                  |< ---------- PREDIS
      |< ---      OUTINP
      |< ---      THRESI
      |< ---      THYDTR
      :                  |< ---------- SOURCE
      :                  |< ---------- REFLOD / REFNQR
      :                  :           |<---------- FCONL
      :                  :           |<---------- NBOIL
      :                  :           |<---------- FRONRF
      :                  :           |<---------- FBOIL
      :                  :           |<---------- FCONG
      :                  :           |<---------- EVAPOR
      :                  |< ---------- HSRINT
      :                  :           |<---------- OXIDAT
      :                  :           |<---------- TFUEA / TFUEP
      :                  :           :           |<---------- SOLVE2
      :                  |< ---------- PRESSU / PRESUN
      :                  :           |<---------- SOLSPA
      :                  |< ---------- FLOVOL
      :                  :           |<---------- VDRIFT
      :                  |< ---------- PREDIS
      :                  |< ---------- CIRCUL
      :                  |< ---------- FLOMAS / FLOMAN
      :                  :           |<---------- SOLSPA
      :                  |< ---------- ENEBAL
      |< ---      OUTTRA
      |< ---      OUTPL1
      |< ---      OUTPL2
      |< ---      THRESO
```

APPENDIX – II: Tasks of the GENFLO modules

Module	Task
GENFLO	Main program for the indepent thermohydraulic and neutronic (RECRIT) solutions. Highest level subroutine in APROS-SA and FRATRAN applications.
RECRE	Assignment of files in the RECRIT and standalone application.
RECFR	Assignment of files in the FRAPTRAN application.
RECSA	Assignment of files in the APROS-SA application.
INITRE	Accident scenario initialization in the RECRIT and standalone application.
INITFR	Accident scenario initialization in the FRAPTRAN application.
INITSA	Accident scenario initialization in the APROS-SA application.
THYDIN	Initialization of the thermohydraulic calculation.
THYDTR	Calculation of a single thermohydraulic time step.
THRESI	Reading termohydraulic restart data.
THRESO	Writing termohydraulic restart data.
INPNOD	Reading and initialization of the thermohydraulic input in the RECRIT and standalone application.
INPFRA	Reading and initialization of the thermohydraulic input in the FRAPTRAN application.
INPAPR	Reading and initialization of the thermohydraulic input in the APROS-SA application.
INPSPE	Reading and initialization of the special component input.
INISPA	Initialization of the sparse matrix solution.
OUTINP	Writing stationary data after the initialization.
SPOOLI	Removing the comment lines from the GENFLO input files.
SOURCE	Coolant source, coolant leak and time dependent energy input.
REFLOD	Wall heat flux and interfacial heat transfer in nodes, with a specific quenching front model.
REFNQR	Wall heat flux and interfacial heat transfer in nodes, quenching front handled by traditional heat transfer correlations without the axially controlled rewetting.
HSRINT	Integration of fuel and cladding temperatures in heat structures.
PRESSU	Solution of the system pressure based on the integral momentum solution.
PRESUN	Solution of the pressure distribution based on the sparse matrix solution.
PREDIS	Solution of the pressure distribution in the integral momentum approach and in the initialization for the PRESUN solution.

CIRCUL	Solution of the integral momentum equation in the integral momentum approach.
FLOVOL	Volumetric flow distribution in the integral momentum approach and the effect of phase separation for mass flow distribution.
FLOMAS	Liquid and vapour mass flow distribution based on the Gauss-Seidel iteration principle.
FLOMAS	Liquid and vapour mass flow distribution applying the sparse matrix solution.
ENEBAL	Mass and enthalpy conservation for vapour and liquid.
OUTTRA	Writing listing output.
OUTPL1	Plotting output for the RECRIT and APROS-SA application.
OUTPL2	Plotting output for the FRAPTRAN application.
FCONV	Convective heat transfer from the surface to liquid.
QCRIT	Critical heat flux on the surface.
NBOIL	Nucleate boiling heat flow and evaporation calculation.
FBOIL	Film boiling heat flow calculation in the dryout conditions.
FCONG	Convective heat transfer from the surface to steam.
FRONFR	Velocity of the rewetting front, heat flow and steam production.
EVAPOR	Interphasial heat flow between gas and liquid by condensation and flashing, heat transfer between superheated steam and liquid.
MATPRO	Specific material property package for the heat capacity and thermal conductance of Zircaloy and UO2.
OXIDAT	Zirconium oxidation in cladding based on the Urbanic-Heidrick model.
TFUEA	Integration of fuel and cladding temperatures, by modelling only the average temperatures for the fuel pellet and cladding.
TFUEP	Integration the detailed distributions of fuel and cladding temperatures.
SOLVE2	Gaussian elimination for a tridiagonal matrix band matrix.
SOLSPA	Gaussian elimination for the sparse matrix.
XINTPL	Linear interpolation of the time dependent boundary conditions for the mass source, mass leak and energy input.
ROWHLS	Water density as a function of saturation enthalpy.
ROWHP	Water density as a function of enthalpy end pressure.
THL	Saturated liquid temperature as a function of enthalpy.
TSUBSI	Subcooled liquid temperature as a function of enthalpy and pressure.
ROGP	Saturated steam density as a function of pressure.
TSATP	Saturation temperature as a function of pressure.
DTSDP	Pressure derivative of saturation temperature.
HGSAT	Saturation enthalpy of steam as a function of pressure.
HLSAT	Saturation enthalpy of steam as a function of pressure.

HEVAP	Evaporation enthalpy as a function of pressure.
DRODP	Pressure derivative of steam density.
DHLDP	Pressure derivative of saturation enthalpy of water.
CONLT	Water conductivity as a function of temperature.
CONGT	Steam conductivity as a function of temperature.
VISLT	Dynamic viscosity of liquid as a function of temperature.
VISGT	Dynamic viscosity of steam as a function of temperature.
CPGSMA	Specific heat of saturated steam as a function of pressure.
CPLSMA	Specific heat of saturated liquid as a function of temperature.
HTL	Enthalpy of saturated water as a function of temperature.
ROWHP2	Water density as a function of enthalpy end pressure.
CPLHP	Specific heat of saturated liquid as a function of enthalpy and pressure.

Published by

Series title, number and report code of publication

VTT Research Notes 2163
VTT–TIED–2163

Author(s)
Miettinen, Jaakko & Hämäläinen, Anitta

Title

GENFLO – A General Thermal Hydraulic Solution for Accident Simulation

Abstract

Thermal hydraulic simulation capability for accident conditions is needed as a part of several programs. Specific thermal hydraulic models are too heavy for simulation, because also the simulation of the rest of the system requires computer resources. The coupling between different physical models may be so complex that the fixed scope system codes are impossible to install for serving the special physical applications. Hence, the GENFLO (=GENeral FLOw) thermal hydraulic model has been developed at VTT for special applications. This report describes the generalised thermal hydraulic model, GENFLO, which at present has been used in three different applications. In RECRIT, the model is coupled the 2-D transient neutronics model TWODIN for calculating the recriticality accidents in the BWR plant. In FRAPTRAN application the model has been coupled with the transient fuel behaviour code FRAPTRAN for making the study of complex fuel transient possible by simulating the sub-channel thermal hydraulics as realistic as possible. In APROS-SA application the model calculates the core thermal hydraulics during the severe accident until the fuel material relocation and pool generation to the bottom of the reactor vessel is simulated.

Keywords
nuclear power plants, nuclear reactors, accidents, simulation, GENFLO, heat transfer, thermal hydraulics, coolants, loss of coolant accidents, dryout

Activity unit
VTT Processes, Tekniikantie 4 C, P.O.Box 1604, FIN–02044 VTT, Finland

ISBN			Project number
951–38–6083–3 (URL: http://www.inf.vtt.fi/pdf/)			
Date	Language	Pages	Price
December 2002	Engl.	75 p. + app. 4 p.	B
Name of project		Commissioned by	
Series title and ISSN		Sold by	
VTT Tiedotteita – Research Notes 1455–0865 (URL: http://www.inf.vtt.fi/pdf/)		VTT Information Service P.O.Box 2000, FIN–02044 VTT, Finland Phone internat. +358 9 456 4404	

Thermal hydraulic simulation capability for accident conditions is needed as a part of several programs. Specific thermal hydraulic models are too heavy for simulation, because also the simulation of the rest of the system requires computer resources. The coupling between different physical models may be so complex that the fixed scope system codes are impossible to install for serving the special physical applications. Hence, the GENFLO (=GENeral FLOw) thermal hydraulic model has been developed at VTT for special applications. This report describes the generalised thermal hydraulic model, GENFLO, which at present has been used in three different applications. In RECRIT, the model is coupled the 2-D transient neutronics model TWODIN for calculating the recriticality accidents in the BWR plant. In FRAPTRAN application the model has been coupled with the transient fuel behaviour code FRAPTRAN for making the study of complex fuel transient possible by simulating the sub-channel thermal hydraulics as realistic as possible. In APROS-SA application the model calculates the core thermal hydraulics during the severe accident until the fuel material relocation and pool generation to the bottom of the reactor vessel is simulated.

Tätä julkaisua myy
VTT TIETOPALVELU
PL 2000
02044 VTT
Puh. (09) 456 4404
Faksi (09) 456 4374

Denna publikation säljs av
VTT INFORMATIONSTJÄNST
PB 2000
02044 VTT
Tel. (09) 456 4404
Fax (09) 456 4374

This publication is available from
VTT INFORMATION SERVICE
P.O.Box 2000
FIN–02044 VTT, Finland
Phone internat. + 358 9 456 4404
Fax + 358 9 456 4374

ISBN 951–38–6083–3
ISSN 1455–0865